Electronic Supplementary Material (ESI) for Physical Chemistry Chemical Physics.

Electronic Supporting Information (ESI)

Proof-of-Principle of a Purine D-A-D' Ligand Based Ratiometric Chemical Sensor Harnessing Complexation Induced Intermolecular PET

Justina Jovaisaite,* Dace Cīrule, Andris Jeminejs, Irina Novosjolova, Māris Turks, Paulius Baronas, Regimantas Komskis, Sigitas Tumkevicius, Gediminas Jonusauskas* and Saulius Jursenas

Table of Contents

Experimental Procedures

1. Materials and Methods

Spectroscopic measurements of compounds **1**, **2**, **3** and **4** were performed in ethyl acetate (EA), dimethoxyethane (DME) and acetonitrile (ACN), with respective dielectric constants (ε) of 6.02, 7.2 and 37.5. All solvents were purchased from Sigma AIdrich and were of spectroscopic or HPLC grade. Solvents of lower polarity could not be used due to low solubility of compounds in non-polar medium. The following salts for the UV and NMR titration experiments were also purchased from Sigma Aldrich: $Cu(MeCN)_4BF_4$, $Fe(ClO_4)_2 \bullet H_2O$, $NaClO_4$, $Ca(ClO_4)_2$, $Ca(ClO_4)_2 \bullet 4H_2O$, $KClO_4$ and $Zn(ClO_4)_2 \bullet 6H_2O$.

Sample of **3** in 1% wt PMMA (poly(methyl methacrylate)) were made by dissolving material and polymer in chloroform. The initial concentration of 40 mg/ml were selected. The mixture was drop-casted on a quartz plate.

1.1 Steady-state (absorption, fluorescence and quantum yield) experiments

The concentrations for fluorescence quantum yield measurements were selected so the absorbance at excitation wavelength would be around 0.05. For absorption and fluorescence measurements (including titration experiments) the initial concentration of compounds was 10^{-5} M. The quartz cells of 1 cm were used.

The absorption spectra were taken with a spectrophotometer Varian-Cary 5G. The fluorescence spectra were performed using a FluoroMax-3 spectrofluorometer.

For titration experiments, the absorption spectra were measured on a UV−vis−near infrared spectrophotometer Lambda 950 (PerkinElmer); fluorescence spectra were measured using a back-thinned CCD spectrometer PMA-11 (Hamamatsu) and a xenon lamp coupled to a monochromator (full width at half-maximum < 10 meV) as an excitation source.

Fluorescence quantum yields were determined by comparative method. The concentrations of studied compounds in solvents and relative standard 9,10-Diphenylanthracene in cyclohexane ($\varphi^{fl} = 0.97$)[1] were selected so that OD would be around 0.05. The fluorescence quantum yields were calculated using:

$$\varphi_s^{fl} = \varphi_0^{fl} \frac{S_s A_0 n_s^2}{S_0 A_s n_0^2}.$$

Where φ_s^{fl} and φ_0^{fl} are the fluorescence quantum yields of the studied samples in solvents and the standard compound as reference, respectively; A_s and A_0 are the absorptions of samples and standard reference compounds, respectively; S_s and S_0 denotes areas underneath the curves of the fluorescence spectra of the sample solution and the standard reference, respectively; and n_s and n_0 are the refraction indices of solvents for the substance under study and the standard compound.

All steady-state fluorescence spectra were obtained by exiting samples to maxima of the lowest-energy absorption bands.

1.2 Time-resolved fluorescence and transient absorption experiments

For time-resolved fluorescence experiments, the concentration of all compounds were 10^{-5} M. The dilute samples in acetonitrile solution were investigated in 1 cm quartz cuvettes. In case of time-resolved fluorescence experiments with $Ca(ClO_4)_2$ and $Zn(ClO_4)_2 \bullet 6H_2O$, the concentration of **3** in acetonitrile was 10^{-5} M adding 0.5 equivalents ($5x10^{-6}$ M) of metal salts dissolved in acetonitrile. The initial concentration of 10^{-3} M of compound **3** and $5x10^{-4}$ M (0.5 equivalents) of $Ca(ClO_4)_2$ and $Zn(ClO_4)_2 \bullet 6H_2O$ in acetonitrile solution was used for femtosecond transient absorption experiments (in 1 mm quartz cuvettes).

Picosecond and nanosecond time-resolved fluorescence lifetimes of compounds **1**, **2**, **3** and **4** were obtained by methods described elsewhere,[2] using two streak camera set-ups.

Time-resolved fluorescence measurements of compound **3** with Ca^{2+} and Zn^{2+} metal ion salts in a picosecond time domain were performed with Streak Scope C10627 detector (Hamamatsu) coupled with femtosecond laser system Pharos-SP and Orpheus.

All time-resolved fluorescence experiments were done by exiting samples to maxima of the lowest-energy absorption bands.

Femtosecond transient absorption measurements were carried out using commercial spectrometer (Harpia, Light Conversion) pumped with wavelength-tunable optical parametric amplifier (Orpheus, Light Conversion) coupled to 190 fs, 10 kHz pulsed laser (Pharos-SP, Light Conversion). Probe source was white light continuum (WLC) pulses generated by focusing the fundamental 1030 nm harmonic in purified water flowing inside quartz cuvette coupled to home-built flow system. Angle between linearly polarized pump and probe pulses was set to approximately 54 degrees. Samples were excited at 320 nm and 350 nm.

The transient absorption measurements were analyzed by fitting decays as described further. The decays were taken at the positions of spectral features of interest in spectral windows not exceeding 2 nm width. All lifetimes were obtained by fitting decays in Origin using an analytical solution of a set of two differential equations:

$$\begin{cases} \frac{dN_1}{dt} = Gauss(\tau, t0) - \frac{N_1}{\tau 1} \\ \frac{dN_2}{dt} = \frac{N_1}{\tau 1} - \frac{N_2}{\tau 2} \end{cases}.$$

Where Gauss(τ,t0) describes the Gaussian shape excitation pulse with FWHM of τ, N1 and N2 are the populations of states. The initial conditions are N1(0)=N2(0)=0. The final kinetic is obtained by:

$$A(t) = A1 * N_1(t) + A2 * N_2(t).$$

1.3 Density Functional Theory (DFT) Calculations

Ground state molecular geometry was optimized and evaluated by employing DFT methodology with a BMK functional at a 6-31g (d,p) basis set level. Spatial one electron HOMO and LUMO orbital distribution and ground to excited state transition energies with appropriate oscillator strengths were compared using BMK functional at a 6-31g (d,p) basis set level in vacuum.

2. Synthesis and product characterization

Yields refer to chromatographically and spectroscopically homogeneous materials. ^{1}H-NMR spectra were recorded at 500 and 300 MHz with internal references from residual non-deuterated solvents (δ 7.26 for $CDCl_3$ and δ 2.50 for DMSO-d_6). ^{13}C-NMR spectra were recorded at 125.7 and 75.5 MHz with internal references from solvent carbon signals (δ 77.1 for $CDCl_3$ and δ 39.5 for DMSO-d_6). Coupling constants were reported in Hz. Infrared spectra were registered using Perkin Elmer Spectrum BX spectrometer and reported in cm^{-1}. Analytical thin layer chromatography (TLC) was performed on Merck silica gel 60 F254 aluminium plates precoated with a 0.25 mm layer of silica gel. For HPLC analyses Agilent Technologies 1200 Series system was used (X Bridge C18 column, 4.6×150 mm, particle size 3.5 µm). Eluent A – 0.01 M KH_2PO_4 water solution/ACN (94/6, V/V), eluent B – ACN. Gradient: 10–95% B 7 min, 95% B 3 min, 95–10% B 2 min. Flow rate: 1 mL/min. Wavelength of detection was set to 260 nm. HRMS analysis was performed on Agilent 1290 Infinity series UPLC system, connected to Agilent 6230 TOF LC/MS mass spectrometer; column Extend C18 RRHD 2.1×50 mm, 1.8 µm. Eluents: formic acid (0.1%) in ACN and formic acid in water (0.1%).

General procedure for the synthesis of 9-(3',5'-di-*O*-acetyl-2'-deoxy-β-D-ribofuranosyl)-2,6-bis-(1*H*-1,2,3-triazol-1-yl)-9*H*-purine derivatives 1-4

Corresponding acetylene (5.0 eq.) and 10% AcOH aqueous solution were subsequently added to a stirred solution of 9-(3',5'-di-*O*-acetyl-2'-deoxy-β-D-ribofuranosyl)-2,6-diazidopurine [3,4] (**A**, 1.0 eq.) in *t*-BuOH (8–100 mL). Then $CuSO_4 \cdot 5H_2O$ and sodium ascorbate were separately dissolved in H_2O (3 mL) and added to the mixture. The reaction mixture was covered with aluminium foil and stirred for 18–24 h at 30–50 °C, controlled by HPLC. Then the reaction mixture was evaporated, dissolved in DCM (60 mL) and washed with saturated $NaHCO_3$ solution (3×15 mL). Organic phase was evaporated, dried *in vacuo* (12 h, 10 Torr) and purified by column chromatography.

9-(3',5'-Di-*O*-acetyl-2'-deoxy-β-D-ribofuranosyl)-2,6-bis-(4-methoxycarbonyl-1*H*-1,2,3-triazol-1-yl)-9*H*-purine (1)

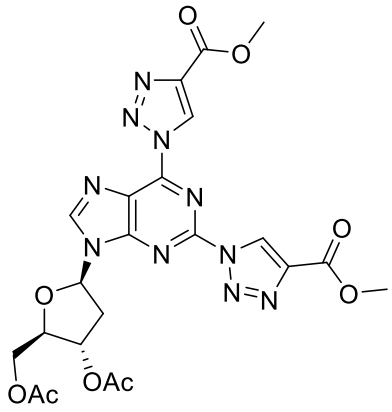

The compound **1** was synthesized according to general procedure: diazide **A** (1.36 g, 3.38 mmol, 1.0 eq.), methylpropiolate (1.66 mL, ρ = 0.945 g/mL, 18.64 mmol, 5.0 eq.), *t*-BuOH (55 mL), 10% AcOH aq. solution (17 mL), $CuSO_4 \cdot 5H_2O$ (102 mg, 0.41 mmol, 12 mol-%), sodium ascorbate (148 mg, 0.75 mmol, 22 mol-%). Reaction conditions: 18 h 35 ºC. Purified with column chromatography (100% ethyl acetate).

Yield: 1.20 g, 62%. Slightly yellow foam, R_f = 0.45 (EtOAc/MeCN = 10/1), t_R = 4.016 min. IR (KBr) ν (cm^{-1}): 3145, 2955, 1740, 1615, 1590, 1480, 1330, 1235, 1030. ^{1}H NMR (300 MHz, $CDCl_3$) δ (ppm): 9.62 (s, 1H, H-C(triazole(6)), 9.28 (s, 1H, H-C(triazole(2))), 8.62 (s, 1H, H-C(8)), 6.71 (dd, 1H, $^{3}J_{1'\text{-}2a'}$ = 7.5 Hz, $^{3}J_{1'\text{-}2b'}$ = 6.1 Hz, H-C(1')), 5.52–5.45 (m, 1H, H-C(3')), 4.52–4.36 (m, 3H, H-C(4'), H_2C(5')), 4.02 (s, 6H, 2×(-CH_3)), 2.94 (ddd, 1H, $^{3}J_{1'\text{-}2a'}$ = 7.5 Hz, $^{2}J_{2a'\text{-}2b'}$ = 14.2 Hz, $^{3}J_{2a'\text{-}3'}$ = 6.7 Hz, Ha-C(2')), 2.85 (ddd, 1H, $^{3}J_{1'\text{-}2b'}$ = 6.1 Hz, $^{2}J_{2a'\text{-}2b'}$ = 14.2 Hz, $^{3}J_{2b'\text{-}3'}$ = 2.8 Hz, Hb-C(2')), 2.18, 2.10 (2s, 6H, H_3CC(O)O-C(3',5')). ^{13}C NMR (75.5 MHz, DMSO-d_6) δ (ppm): 170.08, 170.05, 160.3, 160.1, 155.5, 148.2, 147.0, 144.2, 139.4, 139.2, 129.0, 128.8, 123.4, 84.2, 82.2, 74.1, 63.5, 52.3, 52.1, 35.8, 20.8, 20.5. HRMS (ESI) *m/z* [*M*+H]$^{+}$ calcd for $C_{22}H_{22}N_{10}O_9$: 571.1644; found 571.1653 (1.58 ppm).

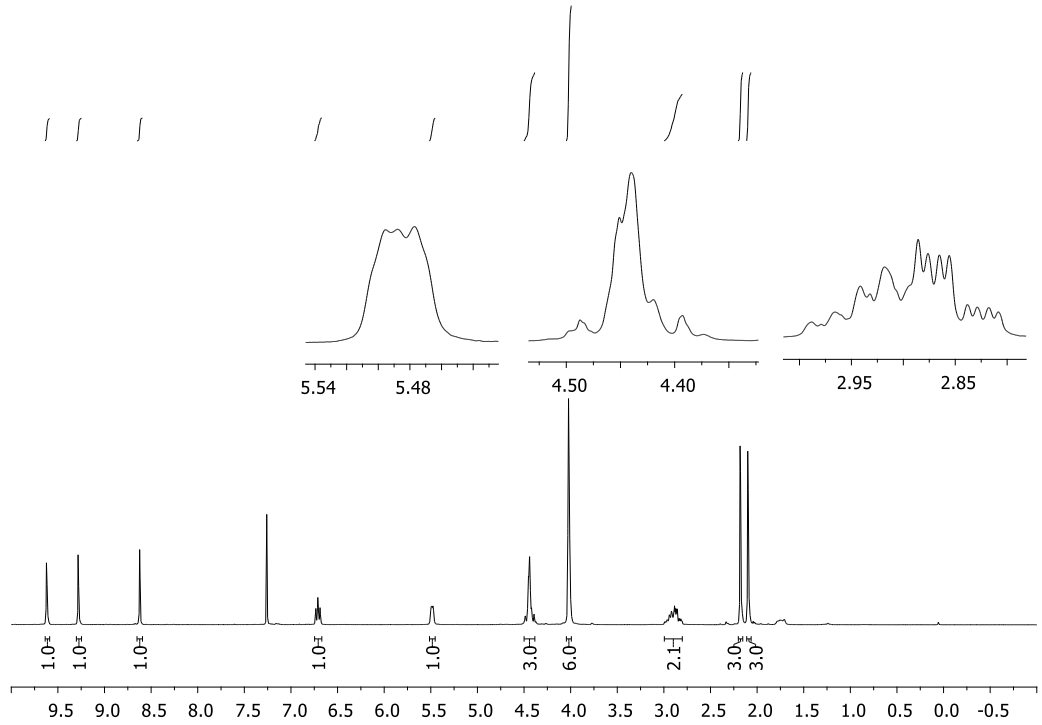

Figure S1. ^{1}H NMR (300 MHz, $CDCl_3$) spectrum of compound **1**.

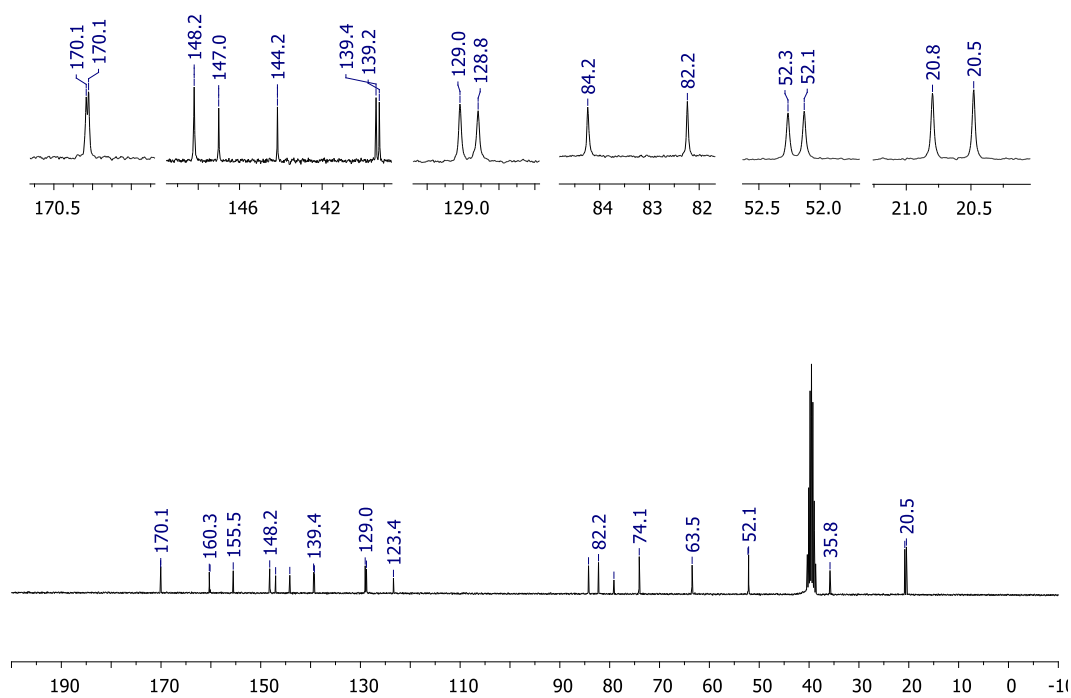

Figure S2. ^{13}C NMR (75.5 MHz, DMSO-d_6) spectrum of compound **1**.

9-(3',5'-Di-*O*-acetyl-2'-deoxy-β-D-ribofuranosyl)-2,6-bis-(4-phenyl-1*H*-1,2,3-triazol-1-yl)-9*H*-purine (2)

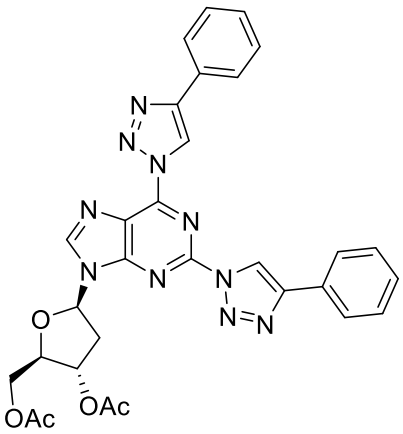

The compound **2** was synthesized according to general procedure: diazide **A** (3.00 g, 7.46 mmol, 1.0 eq.), phenylacetylene (4.10 mL, ρ = 0.930 g/mL, 37.30 mmol, 5.0 eq.), *t*-BuOH (100 mL), 10% AcOH aq. solution (35 mL), $CuSO_4 \cdot 5H_2O$ (307 mg, 1.23 mmol, 17 mol-%), sodium asc. (443 mg, 2.24 mmol, 30 mol-%). Reaction conditions: 24 h 35 ºC. Purified with column chromatography (ACN/Tol; gradient 20%→33%).

Yield: 2.81 g, 62%. Colorless amorphous solid, R_f = 0.67 (ACN/Tol = 1/1), t_R = 6.074 min. IR (KBr) ν (cm^{-1}): 3145, 2945, 1740, 1610, 1585, 1475, 1365, 1230, 1005. ^{1}H NMR (300 MHz, $CDCl_3$) δ (ppm): 9.21 (s, 1H, H-C(triazole(6))), 8.91 (s, 1H, H-C(triazole(2))), 8.45 (s, 1H, H-C(8)), 7.96 (ddd, 4H, ^3J = 8.5 Hz, ^4J = 2.5 Hz, ^5J = 1.4 Hz, Ar), 7.48–7.39 (m, 4H, Ar), 7.39–7.31 (m, 2H, Ar), 6.66 (dd, 1H, $^3J_{1'\text{-}2a'}$ = 7.3 Hz, $^3J_{1'\text{-}2b'}$ = 6.2 Hz, H-C(1')), 5.55 (dt, 1H, $^3J_{2a'\text{-}3'}$ = 6.5 Hz, $^3J_{2b'\text{-}3'}$ = $^3J_{3'\text{-}4'}$ = 2.8 Hz, H-C(3')), 4.48–4.39 (m, 3H, H-C(4'), H_2C(5')), 3.05 (ddd, 1H, $^3J_{1'\text{-}2a'}$ = 7.3 Hz, $^2J_{2a'\text{-}2b'}$ = 14.3 Hz, $^3J_{2a'\text{-}3'}$ = 6.5 Hz, Ha-C(2')), 2.84 (ddd, 1H, $^3J_{1'\text{-}2b'}$ = 6.2 Hz, $^2J_{2a'\text{-}2b'}$ = 14.3 Hz, $^3J_{2b'\text{-}3'}$ = 2.8 Hz, Hb-C(2')), 2.18, 2.07 (2s, 6H, H_3CC(O)O-C(3',5')). ^{13}C NMR (75.5 MHz, $CDCl_3$) δ (ppm): 170.5, 170.4, 155.0, 148.7, 148.4, 148.3, 145.4, 129.7, 129.4, 129.1 (3C)[1], 129.0, 128.8, 126.3, 126.1, 122.6, 119.6, 119.0, 85.2, 83.1, 74.2, 63.7, 38.1, 21.1, 20.9. HRMS (ESI) *m/z* [*M*+H]$^+$ calcd for $C_{30}H_{26}N_{10}O_5$: 607.2160; found 607.2161 (0.16 ppm).

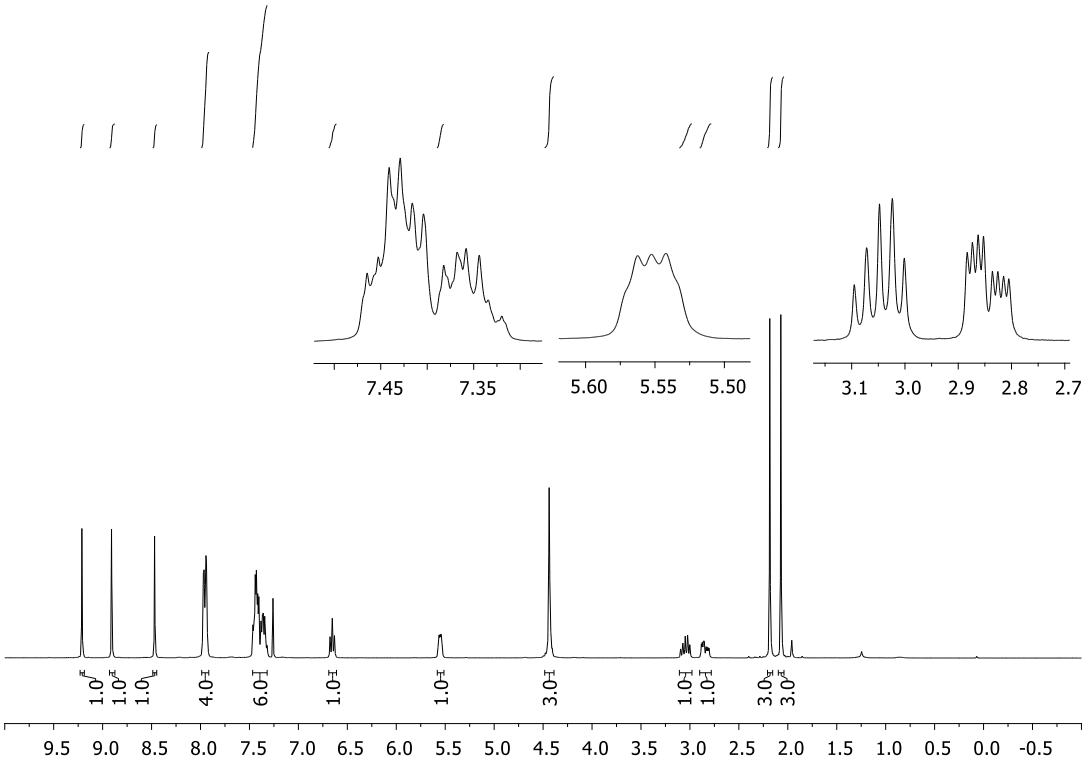

Figure S3. ^{1}H NMR (300 MHz, $CDCl_3$) spectrum of compound **2**.

[1] This signal was assigned from HSQC spectrum.

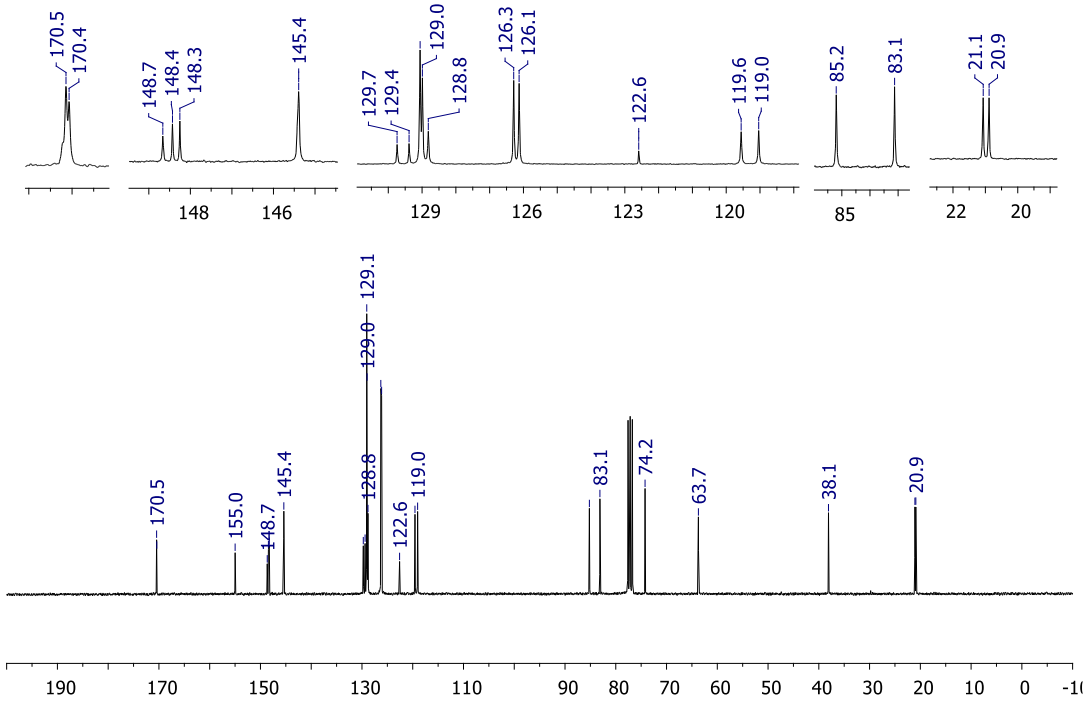

Figure S4. ^{13}C NMR (75.5 MHz, $CDCl_3$) spectrum of compound **2**.

9-(3',5'-Di-*O*-acetyl-2'-deoxy-β-D-ribofuranosyl)-2,6-bis-[4-(4-methoxyphenyl)-1*H*- 1,2,3-triazol-1-yl]-9*H*-purine (3)

The compound **3** was synthesized according to general procedure: diazide **A** (200 mg, 0.50 mmol, 1.0 eq.), 4-methoxy-phenylacetylene (329 mg, 2.49 mmol, 5.0 eq.), *t*-BuOH (8 mL), 10% AcOH aq. solution (5 mL), $CuSO_4 \cdot 5H_2O$ (20 mg, 0.08 mmol, 16 mol-%), sodium ascorbate (31 mg, 0.16 mmol, 32 mol-%). Reaction conditions: 24 h 30 ºC. Purified with column chromatography (ACN/Tol; gradient 15%→33%).

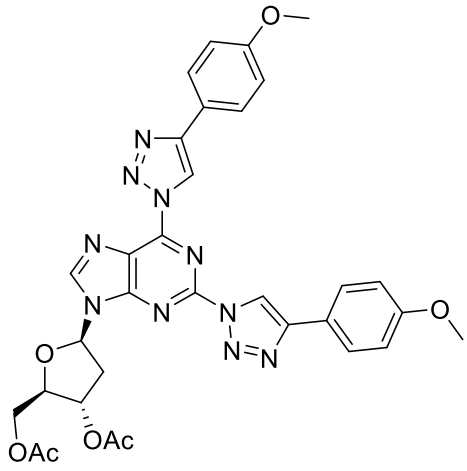

Yield: 250 mg, 75%. Slightly yellow foam, R_f = 0.51 (ACN/Tol = 1/2), t*R* = 5.942 min. IR (KBr) ν (cm^{-1}): 3145, 3000, 2945, 2840, 1740, 1615, 1585, 1455, 1250, 1175, 1015, 1000. ^1H NMR (300 MHz, DMSO-d_6) δ (ppm): 9.61 (s, 1H, H-C(triazole(6))), 9.48 (s, H, H-C(triazole(2))), 9.06 (s, 1H, H-C(8)), 8.00 (d, 2H, ^3J = 7.3 Hz, Ar), 7.98 (d, 2H, ^3J = 7.7 Hz, Ar), 7.08 (d, 2H, ^3J = 7.7 Hz, Ar), 7.07 (d, 2H, ^3J = 7.3 Hz, Ar), 6.64 (dd, 1H, $^3J_{1'\text{-}2a'}$ = 7.3 Hz, $^3J_{1'\text{-}2b'}$ = 6.5 Hz, H-C(1')), 5.60 (dt, 1H, $^3J_{2a'\text{-}3'}$ = 6.7 Hz, $^3J_{2b'\text{-}3'}$ = $^3J_{3'\text{-}4'}$ = 2.9 Hz, H-C(3')), 4.40 (dd, 1H, $^3J_{4'\text{-}5a'}$ = 3.7 Hz, $^2J_{5a'\text{-}5b'}$ = 13.0 Hz, Ha-C(5')), 4.41–4.34 (m, 1H, H-C(4')), 4.32 (dd, 1H, $^3J_{4'\text{-}5b'}$ = 5.0 Hz, $^2J_{5a'\text{-}5b'}$ = 13.0 Hz, Hb-C(5')), 3.82 (s, 6H, 2×(-CH_3)), 3.27 (ddd, 1H, $^3J_{1'\text{-}2a'}$ = 7.3 Hz, $^2J_{2a'\text{-}2b'}$ = 14.4 Hz, $^3J_{2a'\text{-}3'}$ = 6.7 Hz, Ha-C(2')), 2.76 (ddd, 1H, $^3J_{1'\text{-}2b'}$ = 6.5 Hz, $^2J_{2a'\text{-}2b'}$ = 14.4 Hz, $^3J_{2b'\text{-}3'}$ = 2.9 Hz, Hb-C(2')), 2.16, 1.99 (2s, 6H, $H_3CC(O)O$-C(3',5')). ^{13}C NMR (75.5 MHz, DMSO-d6) δ (ppm): 170.2 (2C)*, 159.7, 159.5, 155.2, 147.6, 147.5, 146.95, 146.87, 144.7, 127.2, 127.0, 122.7, 122.2, 121.8, 119.3 (2C)[2], 114.5, 114.4, 84.2, 82.2, 74.1, 63.5, 55.2 (2C)*, 35.7, 20.8, 20.5. HRMS (ESI) *m/z* [*M*+H]$^+$ calcd for $C_{32}H_{30}N_{10}O_7$: 667.2383; found 667.2375 (1.20 ppm).

[2] These signals were assigned from HSQC spectrum.

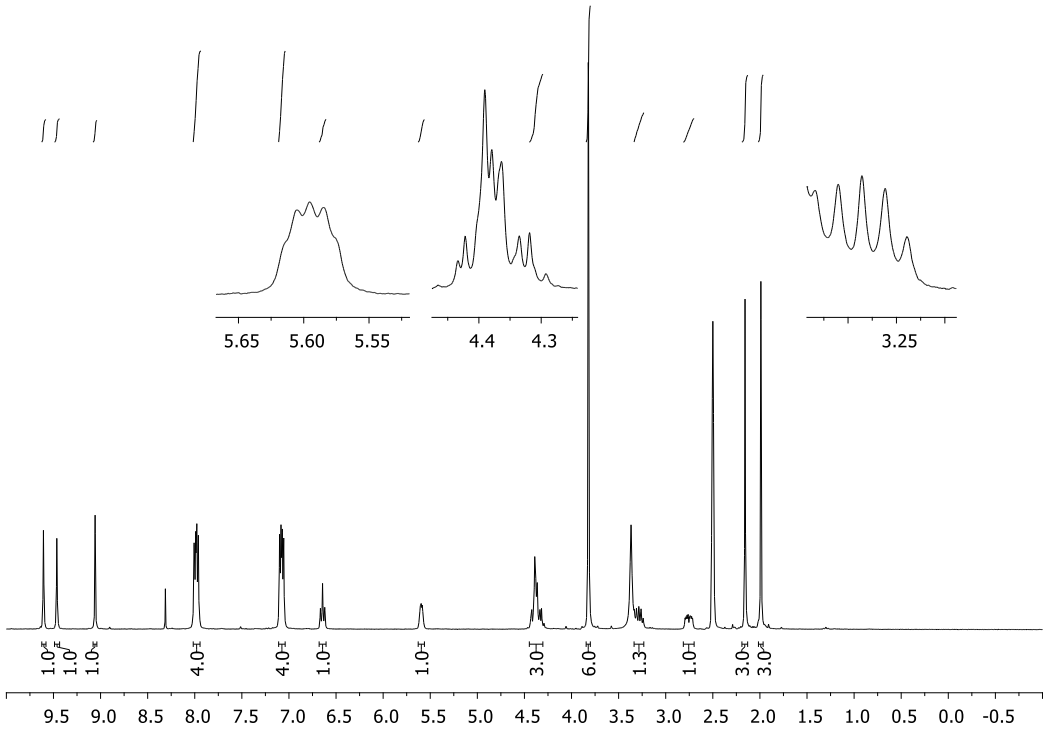

Figure S5. ^{1}H NMR (300 MHz, DMSO-d_6) spectrum of compound **3**.

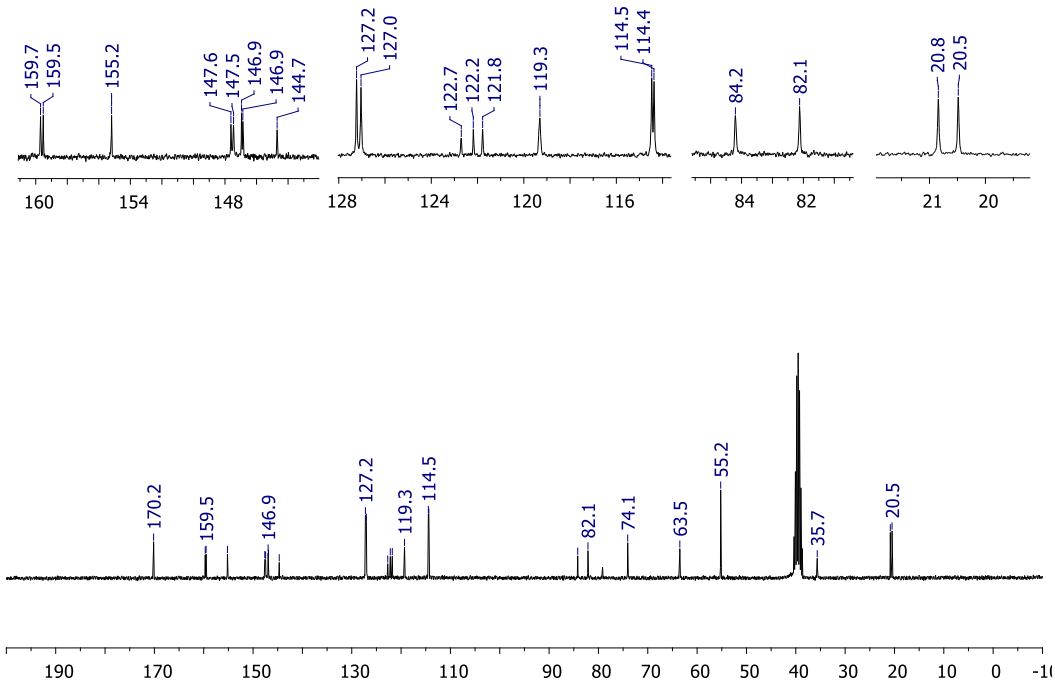

Figure S6. ^{13}C NMR (75.5 MHz, DMSO-d_6) spectrum of compound **3**.

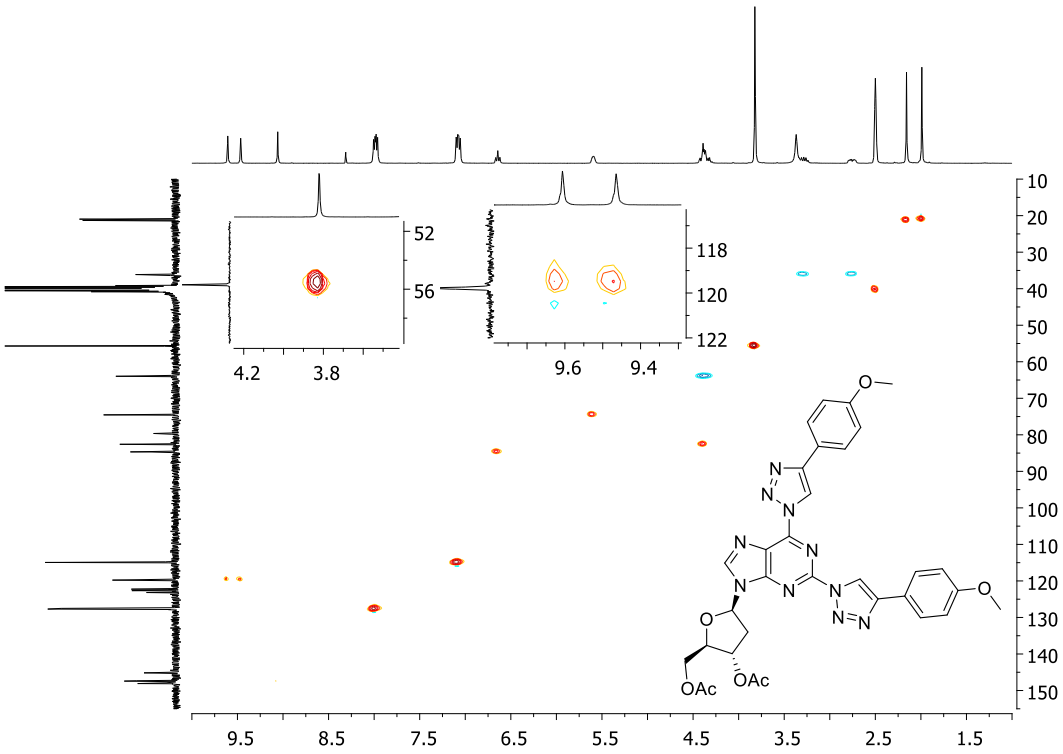

Figure S7. HSQC spectrum of compound **3**.

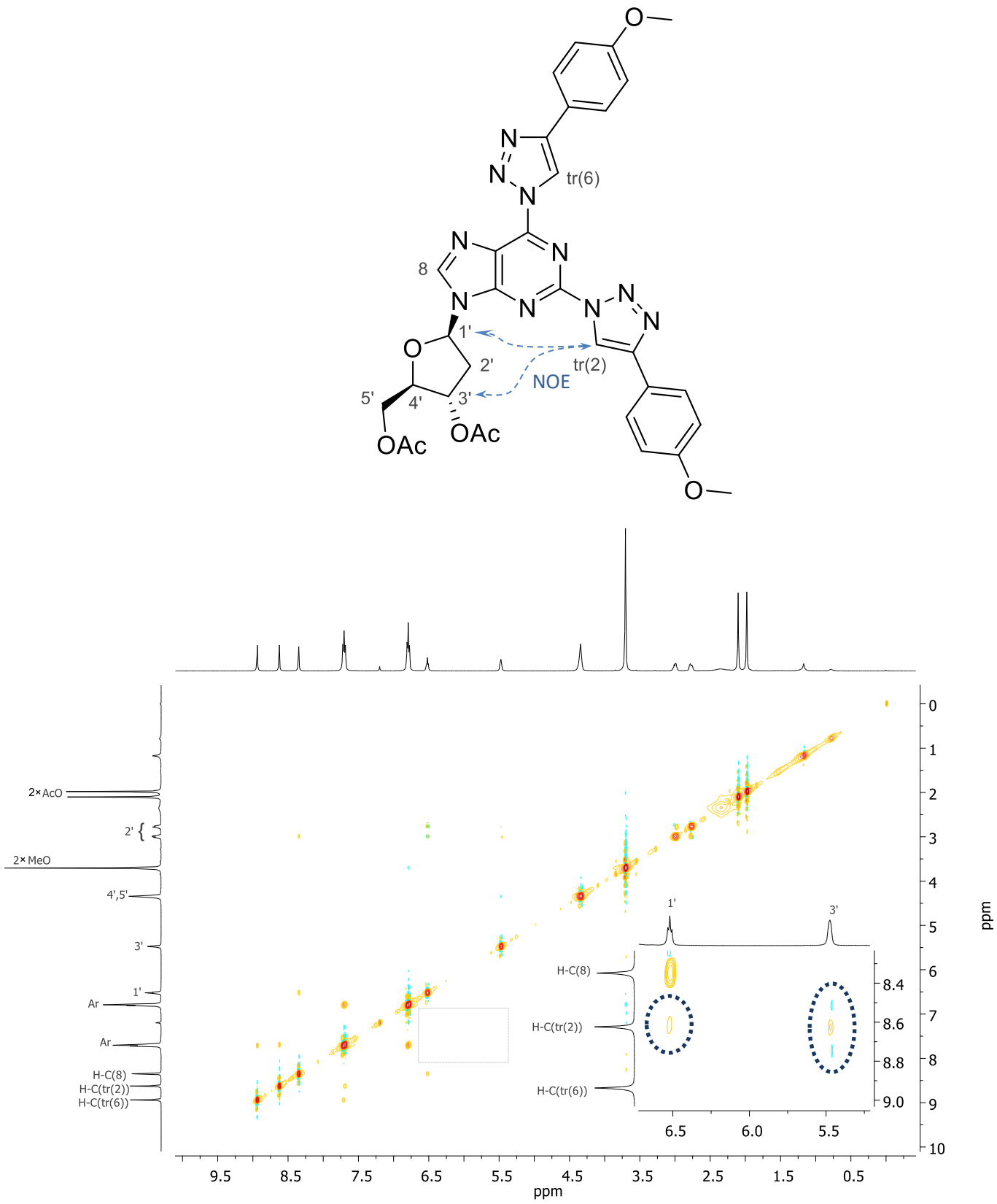

Figure S8. NOESY spectrum of compound **3** (500 MHz, $CDCl_3$).

9-(3',5'-Di-*O*-acetyl-2'-deoxy-β-D-ribofuranosyl)-2,6-bis-[4-(4-dimethylamino-phenyl)-1*H*-1,2,3-triazol-1-yl]-9*H*-purine (4)

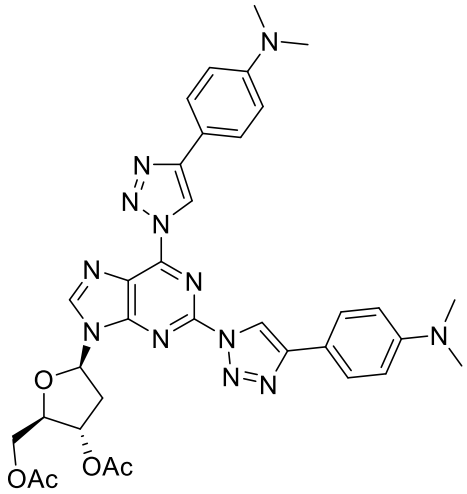

The compound **4** is synthesized according to general procedure: diazide **A** (735 mg, 1.83 mmol, 1.0 eq.), 4'-dimethyl-aminophenylacetylene (1.06 g, 7.31 mmol, 4.0 eq.), *t*-BuOH (25 mL), 10% AcOH aq. solution (8 mL), $CuSO_4 \cdot 5H_2O$ (25 mg, 0.10 mmol, 6 mol-%), sodium ascorbate (36 mg, 0.18 mmol, 10 mol-%). Reaction conditions: 24 h 50 ºC. Purified with column chromatography (ACN/Tol; gradient 9%→40%).

Yield: 200 mg, 16 %. Yellow solid. R_f = 0.64 (ACN/Tol 1:1). ^{1}H NMR (500 MHz, $CDCl_3$) δ (ppm): 9.07(s, H, H-C(triazole(6))), 8.76 (s, H, H-C(triazole(2))), 8.48 (s, 1H, H-C(8)), 7.85 (d, 2H, ^3J = 8.5 Hz, Ar), 7.83 (d, 2H, ^3J = 8.5 Hz, Ar), 6.77 (d, 2H, ^3J = 8.5 Hz, Ar), 6.76 (d, 2H, ^3J = 8.5 Hz, Ar), 6.66 (dd, 1H, $^3J_{1'\text{-}2a'}$ = 7.2 Hz, $^3J_{1'\text{-}2b'}$ = 5.9 Hz, H-C(1')), 5.54 (dt, 1H, $^3J_{2a'\text{-}3'}$ = 6.7 Hz, $^3J_{2b'\text{-}3'}$ = $^3J_{3'\text{-}4'}$ = 2.9 Hz, H-C(3')), 4.49–4.40 (m, 3H, H-C(4'), H_2-C(5')), 3.05–3.01 (m, 1H, Ha-C(2')), 3.00 (2s, 12H, 4×(-CH_3)), 2.85 (ddd, 1H, $^3J_{1'\text{-}2b'}$ = 5.9 Hz, $^2J_{2a'\text{-}2b'}$ = 14.1 Hz, $^3J_{2b'\text{-}3'}$ = 2.9 Hz, Hb-C(2')), 2.18, 2.09 (2s, 6H, $H_3CC(O)O$-C(3',5')). ^{13}C NMR (75.5 MHz, $CDCl_3$) δ (ppm): 170.51, 170.49, 155.0, 150.9, 150.7, 148.93, 148.88, 148.7, 145.6, 144.9, 127.3, 127.1, 122.4, 117.5, 117.2, 112.5 (4C)[3], 85.1, 83.1, 74.4, 63.8, 40.6, 40.5, 38.2, 21.1, 21.0. HRMS (ESI) *m*/*z* [*M*+Na]$^+$ calcd for $C_{34}H_{36}N_{12}O_5$: 715.2829; found 715.2809 (2.80 ppm).

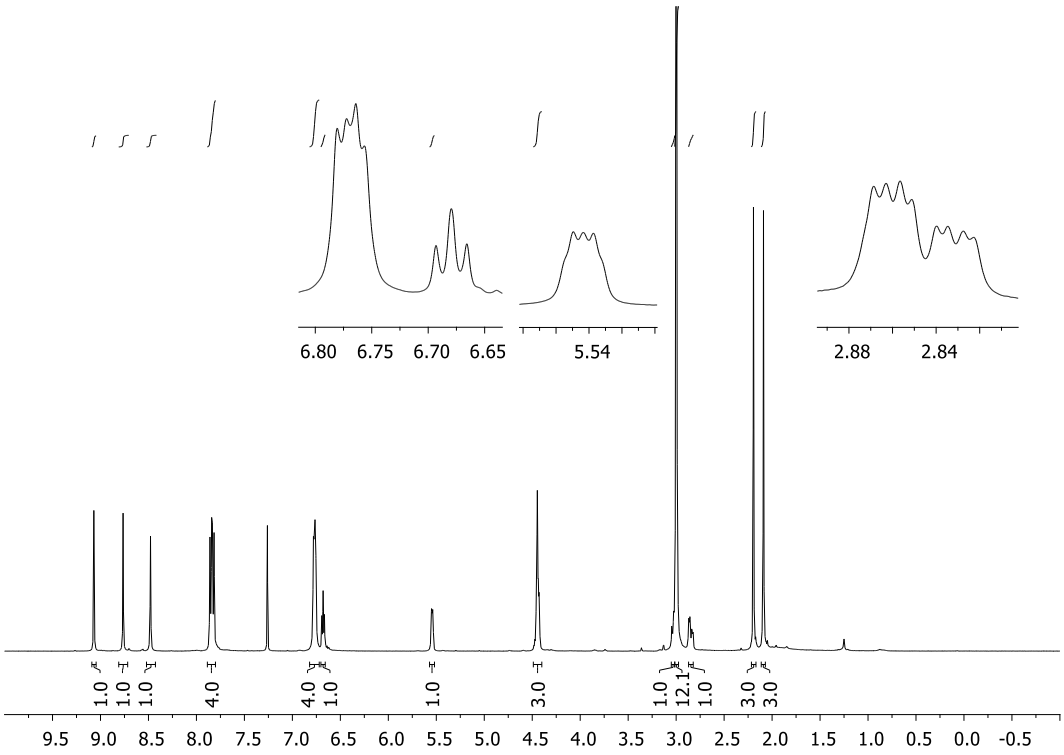

Figure S9. ^{1}H NMR (500 MHz, $CDCl_3$) spectrum of compound **4**.

[3] This signal was assigned from HSQC spectrum.

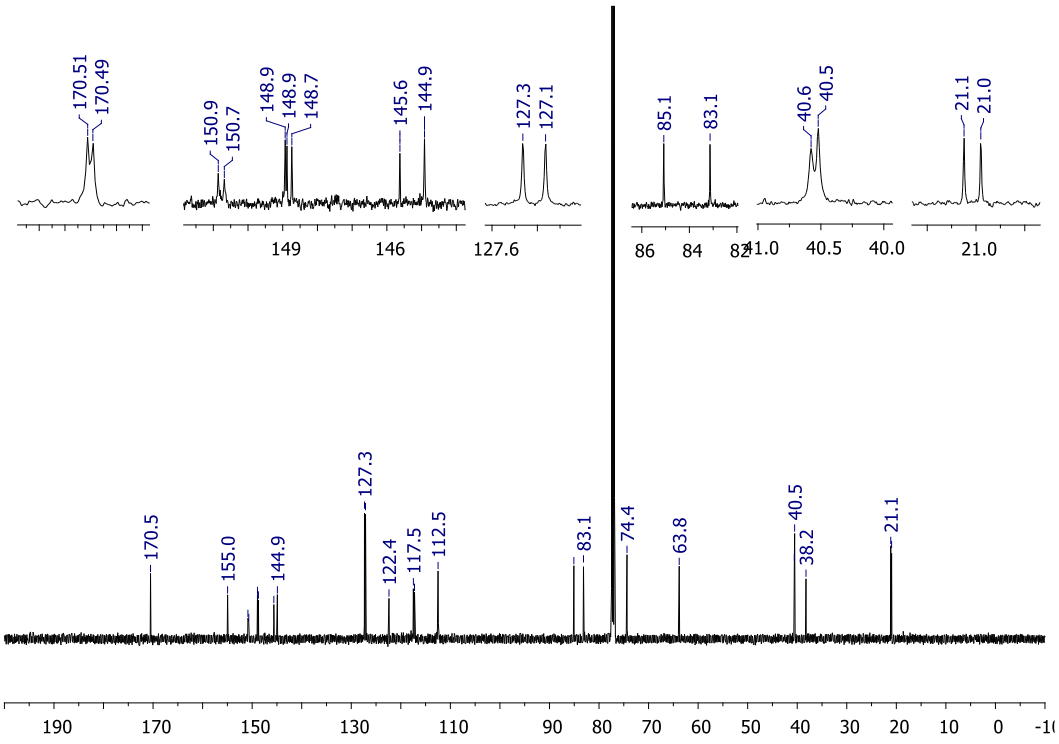

Figure S10. ^{13}C NMR (125.7 MHz, $CDCl_3$) spectrum of compound **4**.

Tautomeric mixture of 7-heptyl-7*H*-tetrazolo[1,5-*i*]purine (5-T) and 6-azido-7-heptyl-9*H*-purine (5-A)

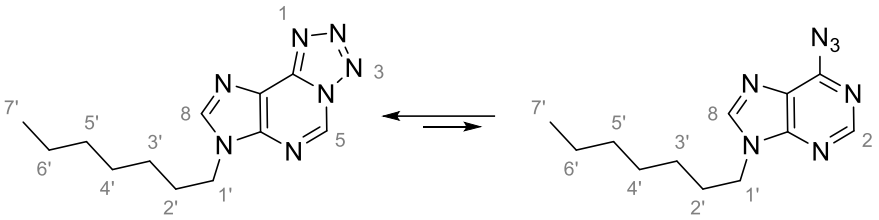

n-Heptyl alcohol (2.2 mL, ρ = 0.82 g/mL, 15.5 mmol, 1.2 eq.) was added to solution of 6-chloropurine (2.0 g, 12.9 mmol, 1.0 equiv.) and triphenylphosphine (4.4 g, 16.8 mmol, 1.3 eq.) in anhydrous THF (20 mL) under argon. This mixture was cooled to 0 °C in NaCl-ice bath. DIAD (3.3 mL, ρ = 1.03 g/mL, 16.8 mmol, 1.3 eq.) was then added in small portions (0.25 mL). In this stage temperature was not allowed to exceed 4 °C and the whole amount of DIAD was added in one hour. Afterwards the reaction vessel was stirred at r.t. for another hour. The volatiles were evaporated and the oily residue was suspended in DMF (10 mL). Sodium azide (1.7 g, 25.9 mmol, 2.0 eq.) was added and the mixture was stirred at 50°C for 24 hours. After completion of the reaction the mixture was suspended in EtOAc (50 mL) and washed with brine (5×10 mL) and water (3×5 mL). The organic phase was dried with anh. Na_2SO_4, filtered, evaporated, crystallised from cold hexane (50 mL) and dried *in vacuo* (12 h, 10 Torr) to yield 1.78 g (53%) of compound **5**.

Only the tetrazole form was characterized from a 35 : 65 mixture of **5-A/5-T:**

^1H NMR ($CDCl_3$, 300 MHz, 25 °C) δ (ppm): 9.49 (s, 1H, H-C(5)), 8.17 (s, 1H, H-C(7)), 4.41 (t, 2H, ^3J = 7.2 Hz, H_2-C(1')), 1.98 (quintet, 2H, ^3J = 7.2 Hz, H_2-C(2')), 1.39–1.29 (m, 8H, 4×(-CH_2-)), 0.87 (t, 3H, ^3J = 6.9 Hz, (-CH_3)). Spectral data matches with literature.[5]

9-heptyl-6-[4-(4-methoxyphenyl)-1*H*-1,2,3-triazol-1-yl]-9*H*-purine (6)

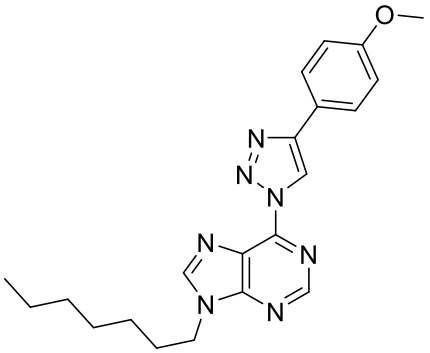

Corresponding acetylene (1.79 mmol, 2.0 eq.), acetic acid (60 µL, 0.98 mmol, 1.1 eq.) and triethylamine (0.14 mL, ρ = 0.73 g/mL, 0.98 mmol, 1.1 eq.) were subsequently added to stirred solution of **5** (0.23 g, 0.89 mmol, 1.0 eq.) in DCM (15 mL). Then copper (I) iodide (25 mg, 0.13 mmol, 15 mol-%) was added and the misture was stirred at room temperature for 24 hours. After the completion of the reaction the mixture was washed with $NaHS/H_2O$ solution (5×3 mL) and the organic phase was dried with anh. Na_2SO_4, filtered, evaporated, and recrystallised from hexane (≈70 mL) and dried *in vacuo* (12 h, 10 Torr) to yield 0.13 g (37%) of compound **6**.

Slightly yellow solid, R_f = 0.85 (DCM/MeOH 4:1). ^{1}H NMR (500 MHz, $CDCl_3$) δ 9.22 (s, 1H, H-C(triazole), 8.96 (s, 1H, H-C(2)), 8.24 (s, 1H, H-C(8)), 7.94 (d, 2H, ^3J = 8.6 Hz, 2×H-C(Ar)), 7.01 (d, 2H, ^3J = 8.6 Hz, 2×H-C(Ar)), 4.36 (t, 2H, ^3J = 7.2 Hz, H_2-C(1')), 3.87 (s, 3H, (-OMe))), 1.98 (quintet, 2H, ^3J = 7.2 Hz, H_2-C(2')), 1.40–1.25 (m, 8H, 4×(-CH_2-)), 0.87 (t, 3H, ^3J = 6.8 Hz, (-CH_3)). ^{13}C NMR (125.7 MHz, $CDCl_3$) δ 160.2, 154.7, 152.3, 148.2, 146.0, 145.0, 127.7, 122.8, 122.7, 118.8, 114.5, 55.5, 44.6, 31.7, 30.0, 28.8, 26.7, 22.6, 14.1. HRMS (ESI) *m/z* $[M+H]^+$ calcd for $C_{21}H_{26}N_7O$: 392.2193; found 392.2187 (1.53 ppm).

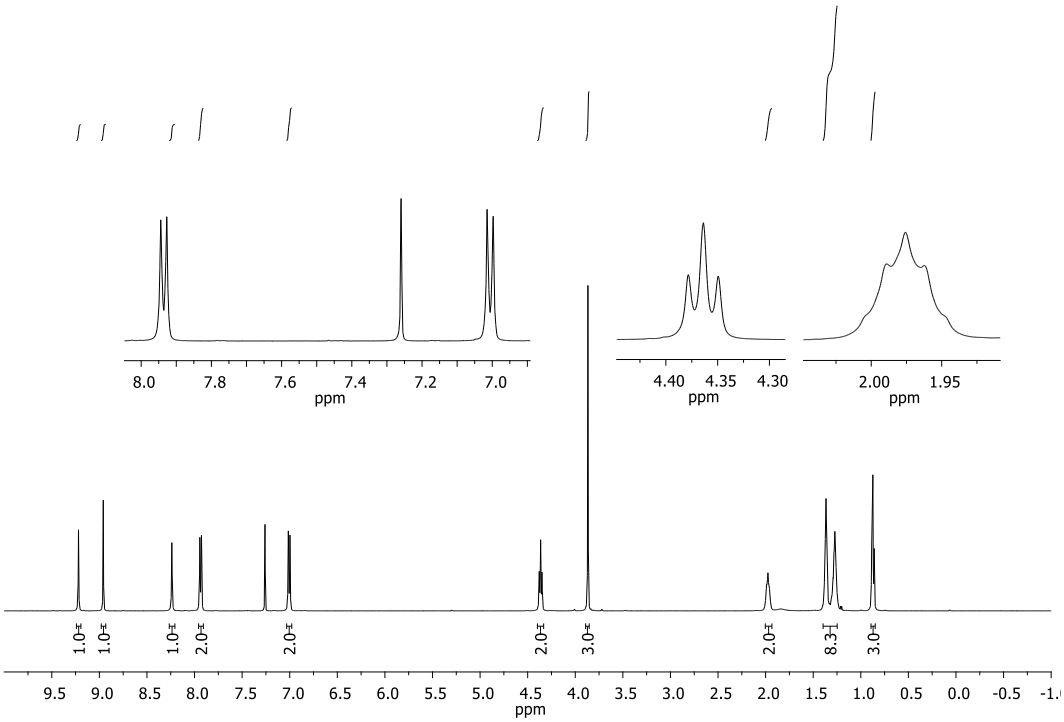

Figure S11. ^{1}H NMR (500 MHz, $CDCl_3$) spectrum of compound **6**.

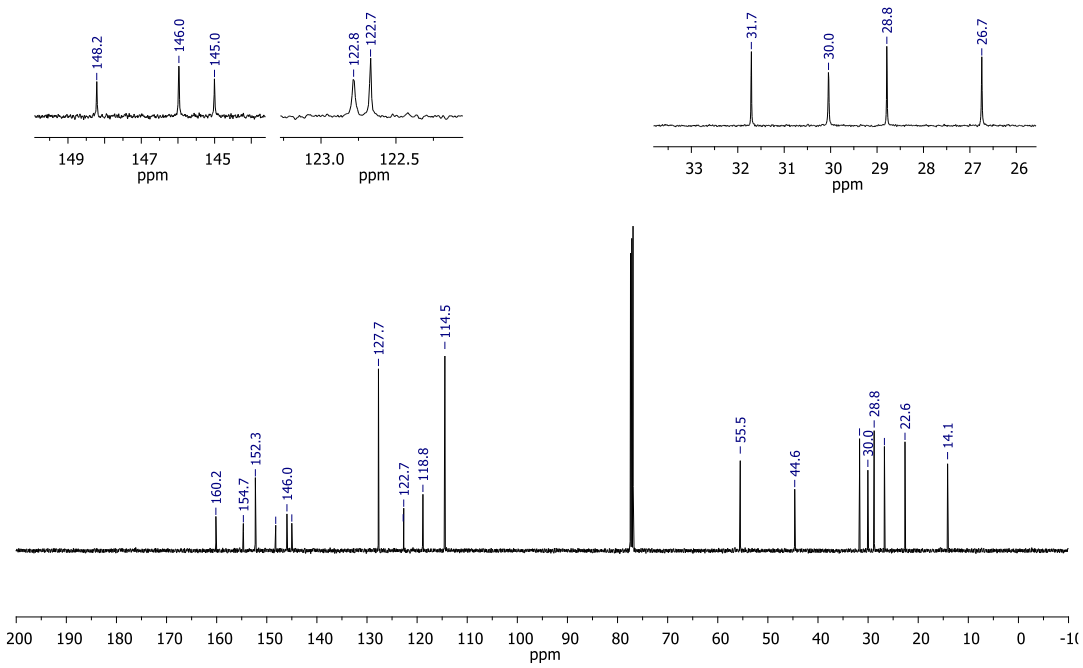

Figure S12. ^{13}C NMR (125.7 MHz, $CDCl_3$) spectrum of compound **6**.

Results

3. Optical properties

No aggregation of ligands was observed at concentrations, used to obtain the experimental results that are presented in this paper.

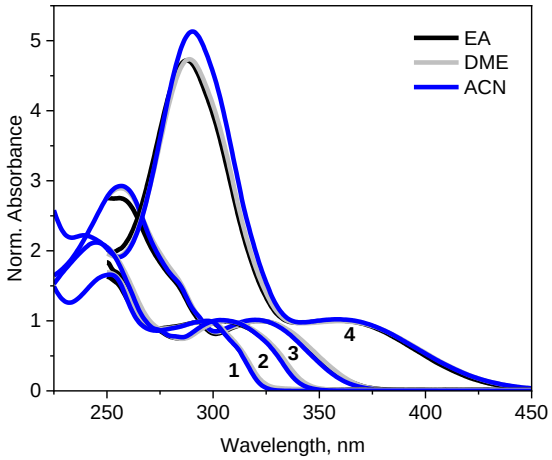

Figure S13. Absorption spectra normalized to maxima of red-side absorption bands of compounds **1**, **2**, **3** and **4** (from left to right) in solutions of different dielectric constants: ethyl acetate (EA), dimethoxyethane (DME) and acetonitrile (ACN).

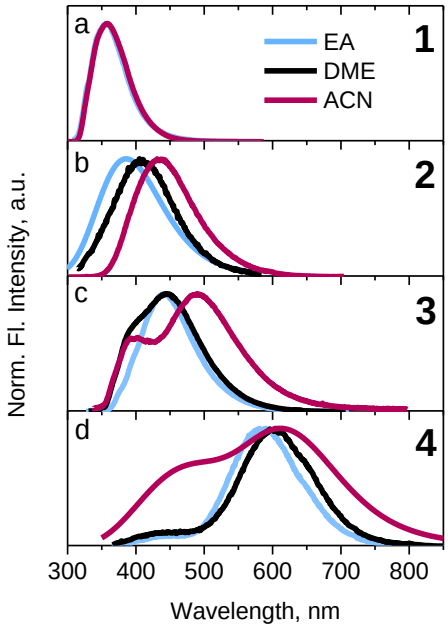

Figure S14. Normalized fluorescence spectra of **1** (a), **2** (b), **3** (c) and **4** (d) in EA, DME and ACN. Represented spectra of compound **2** in EA and **4** in ACN are sums of two Gaussian peak functions (see Figure S15 for original spectra).

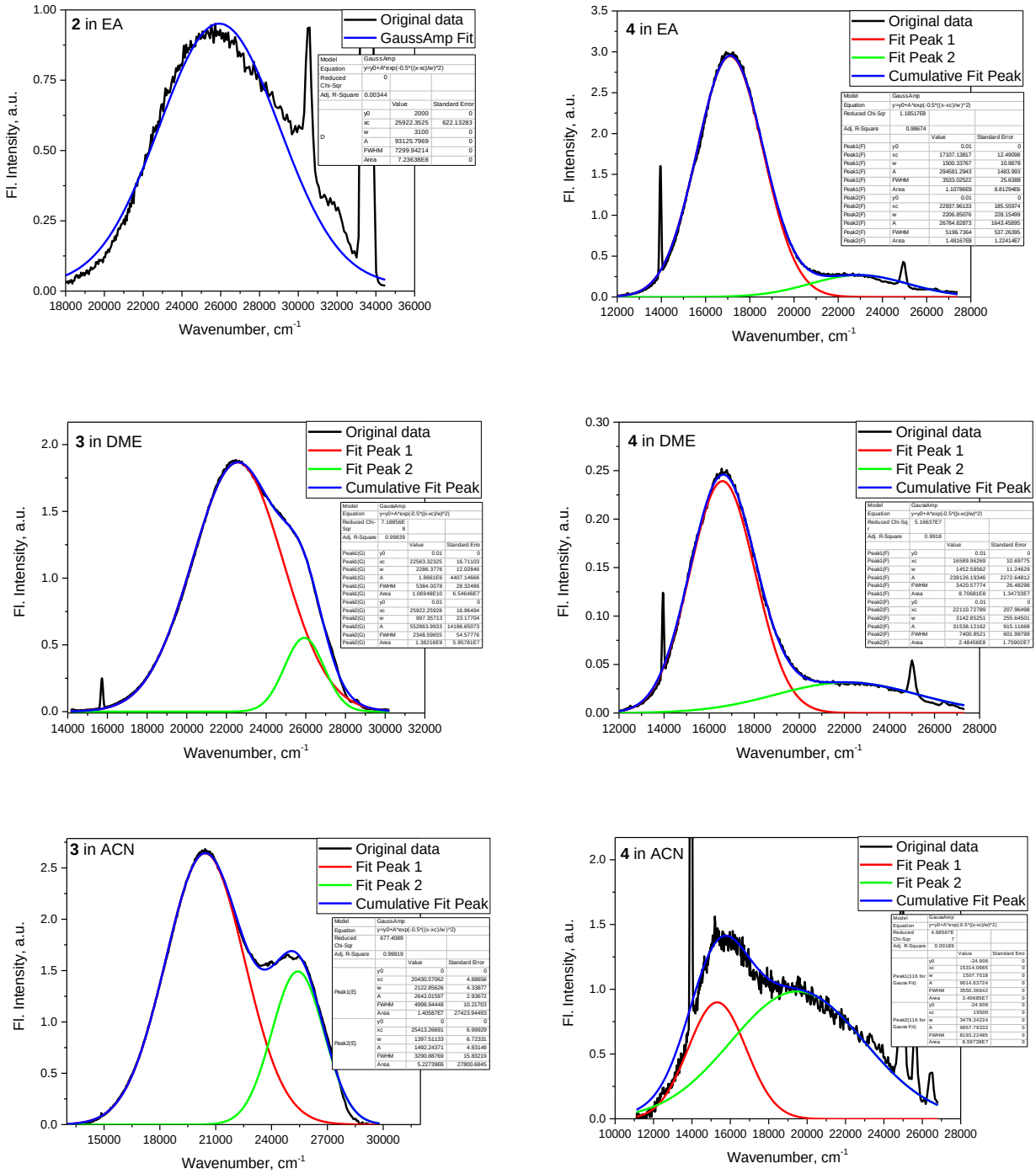

Figure S15. Two Gaussian peak function fits (decomposition) of fluorescence spectra of compounds **2**, **3** and **4** in EA, DME, ACN.

Table S1. Fluorescence decay lifetimes of compounds **1**, **2**, **3** and **4** in ACN.

Compound	Fitted at	τ_1, ns	τ_2, ns
1	358 nm	0.79	1.77
2	390 nm	0.057	0.84
	432 nm	0.16	3.41
3	390 nm		2.41
	480 nm		4.40
3 + 0.5Ca^{2+}	480 nm		4.57
3 + 0.5Zn^{2+}	480 nm		4.44
4	450 nm	0.56	6.00
	645 nm	0.31	2.71

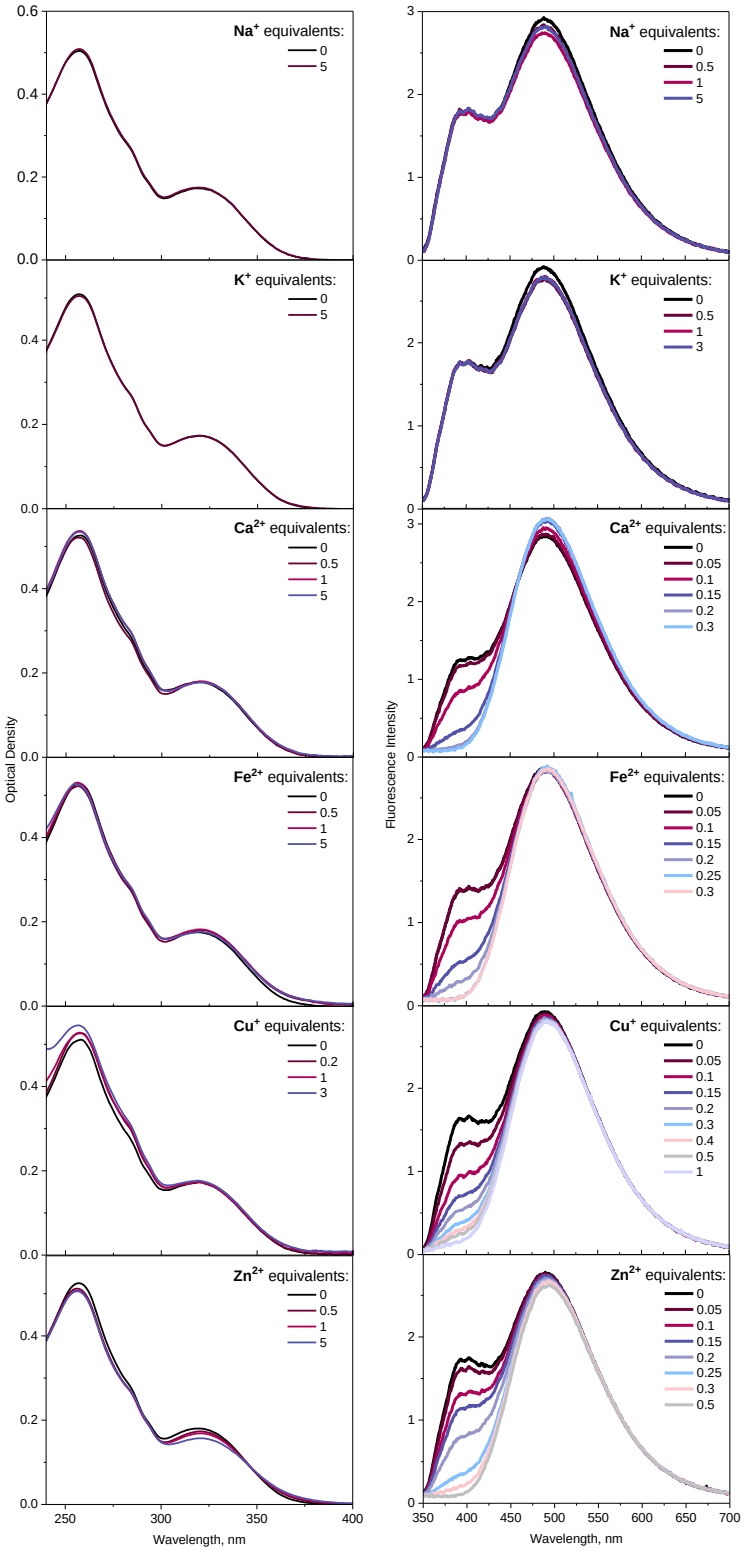

Figure S16. Absorption (left) and fluorescence (right) spectra of **3** upon titration with different metal ions from top to bottom : Na^{+}, K^{+}, Ca^{2+}, Fe^{2+}, Cu^{+}, Zn^{2+}. The equivalents of metal ions in the solution with **3** (ACN, 10^{-5} M) are given in legends of each graph. Excited at 320 nm.

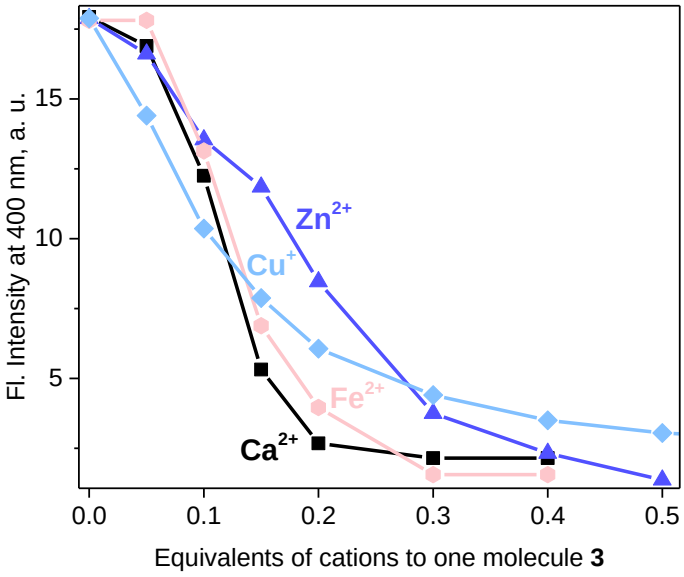

Figure S17. The response of **3** "blue" branch emission (recorded at 400 nm) to metal ion equivalents in ACN. Initial concentration of **3** is 10^{-5} M, excited at 320 nm.

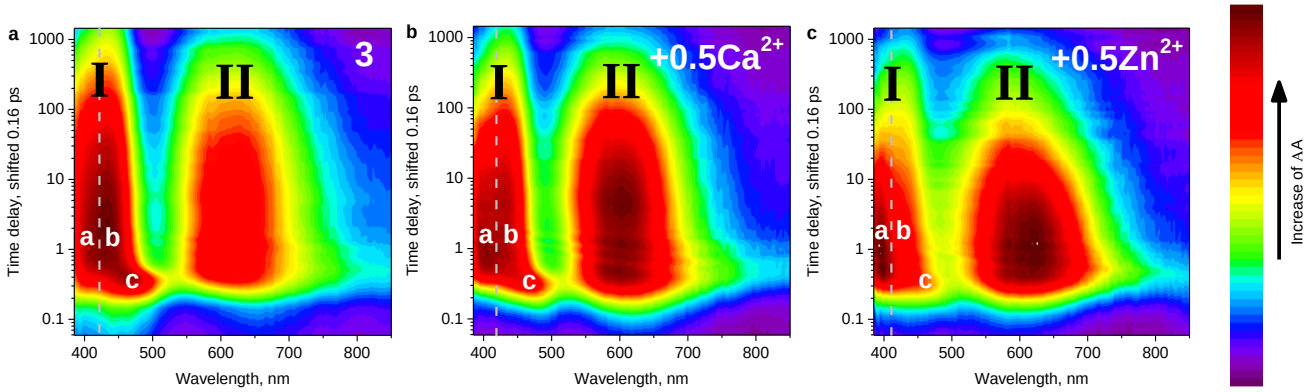

Figure S18. Transient absorption maps of molecule **3** (a), molecule **3** and 0.5 equivalent of Ca^{2+} (b), molecule **3** and 0.5 equivalent of Zn^{2+} (c), obtained by exciting samples at 320 nm. All samples were dissolved in ACN. Initial concentration of **3** was 10^{-3} M. Two main positive absorption regions are marked as region **I** and region **II**. White letters **a**, **b** and **c** denotes different absorption bands in region **I**.

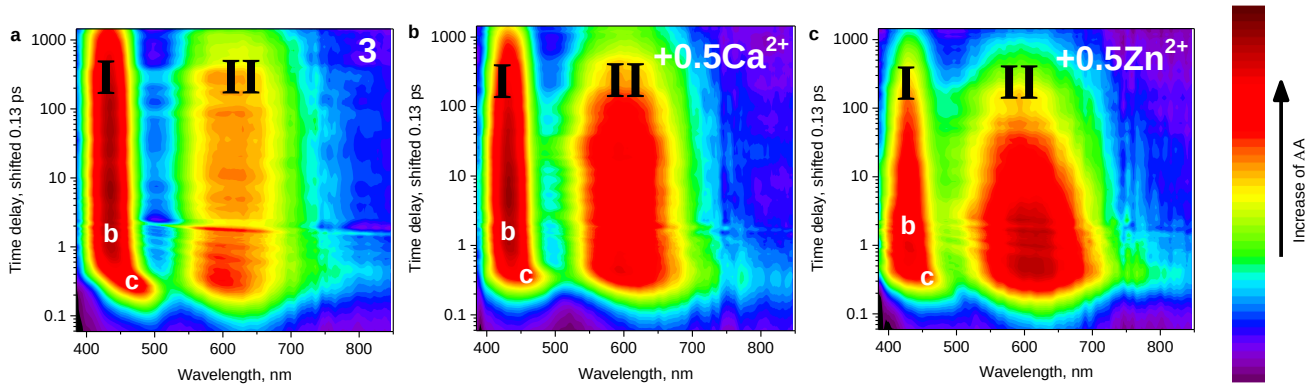

Figure S19. Transient absorption maps of molecule **3** (a), molecule **3** and 0.5 equivalent of Ca^{2+} (b), molecule **3** and 0.5 equivalent of Zn^{2+} (c), obtained by exciting samples at 350 nm. All samples were dissolved in ACN. Initial concentration of **3** was 10^{-3} M. Two main positive absorption regions are marked as region **I** and region **II**. White letters **b** and **c** denotes different absorption bands in region **I**.

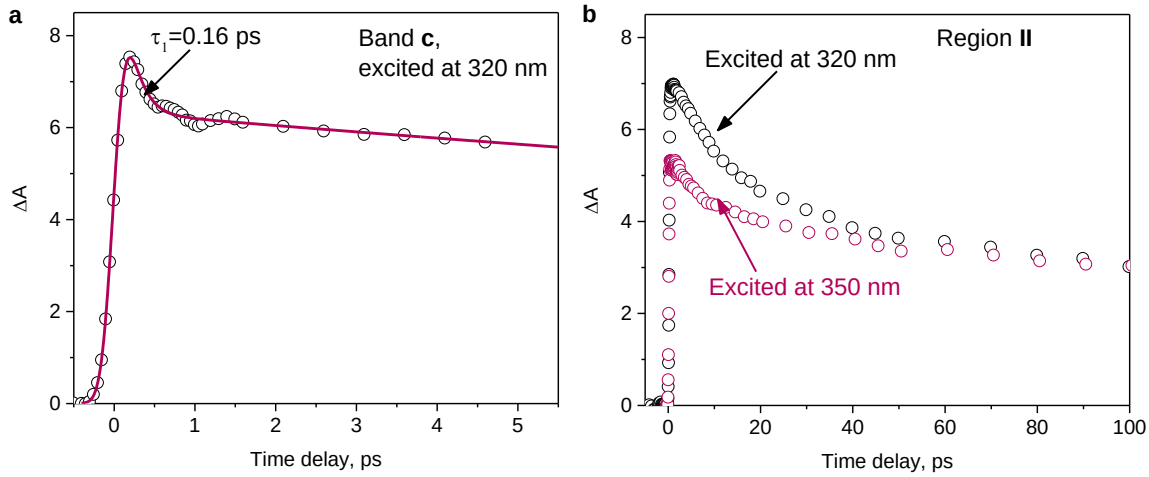

Figure S20. Transient absorption decays of compound **3** without metal salts obtained at band **c** (465 nm) by exciting at 320 nm (a) and of compound **3** with 0.5 equivalent of Zn^{2+} in region **II** (620 nm) by exciting at both 320 nm and 350 nm wavelengths (b). One notice a slight overlap of excitation spectra for the "red" and "blue" branches at 350 nm in (b).

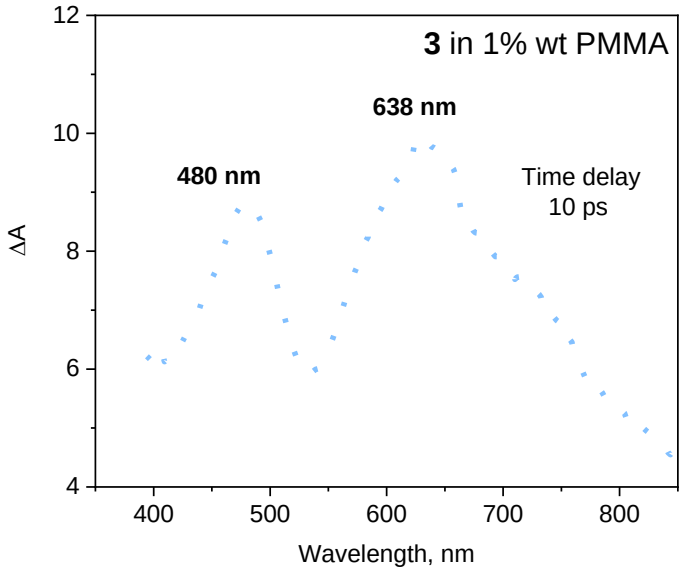

Figure S21. Transient absorption spectra of compound **3** in 1% wt PMMA matrix, recorded at 10 ps delay. Excitation wavelength 320 nm.

4. Theoretical calculations

Table S2. Fundamental molecular orbitals and their energies, optical transition energies and appropriate oscillator strengths of compound **1** in optimized ground state geometry. The geometry optimization as well as optical transition properties were evaluated with DFT approximation and BMK functional at 6-31g (d,p) basis set level in vacuum.

HOMO	LUMO	Transition energy (eV)	Oscillator strength
-7.99 eV 	-1.96 eV 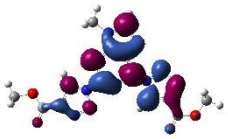	4.59	0.331
HOMO → LUMO (LE_1)			
-7.99 eV 	-1.11 eV 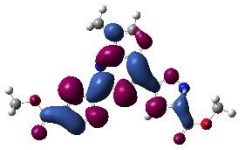	5.06	0.123
HOMO → LUMO+1 (LE_2)			
-9.26 eV 	-1.96 eV 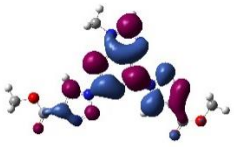	5.67	0.227
HOMO-1 → LUMO (LE_3)			
-9.84 eV 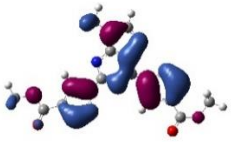	-1.96 eV 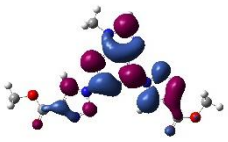	6.11	0.173
HOMO-2 → LUMO (LE_4)			
-7.99 eV 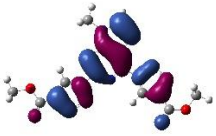	+0.02 eV 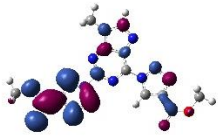	6.52	0.154
HOMO → LUMO+2 (CT_1)			
-9.26 eV 	-1.11 eV 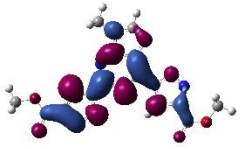	6.61	0.126
HOMO-1 → LUMO+1 (LE_5)			
-7.99 eV 	+0.10 eV 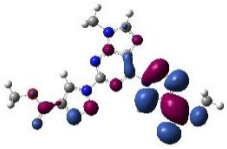	6.65	0.238
HOMO → LUMO+3 (CT_2)			

Table S3. Fundamental molecular orbitals and their energies, optical transition energies and appropriate oscillator strengths of compound **2** in optimized ground state geometry. The geometry optimization as well as optical transition properties were evaluated with DFT approximation and BMK functional at 6-31g (d,p) basis set level in vacuum.

HOMO	LUMO	Transition energy (eV)	Oscillator strength
-6.80 eV 	-1.54 eV 	4.04	0.353
HOMO ("Red" branch donor) → LUMO (Purine acceptor) (CT_1)			
-6.92 eV 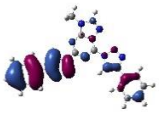	-1.54 eV 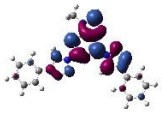	4.27	0.333
HOMO-1 ("Blue" branch donor) → LUMO (Purine acceptor) (CT_2)			
-6.80 eV 	-0.73 eV 	4.75	0.280
HOMO ("Red" branch donor) → LUMO+1 (Purine acceptor) (CT_3)			
-6.92 eV 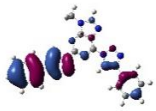	-0.73 eV 	4.75	0.280
HOMO-1 ("Blue" branch donor) → LUMO+1 (Purine acceptor) (CT_4)			
-7.88 eV 	-1.54 eV 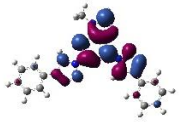	4.90	0.183
HOMO-2 (Purine acceptor) → LUMO (Purine acceptor) (LE_1)			
-8.78 eV 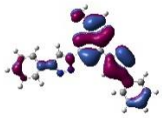	-1.54 eV 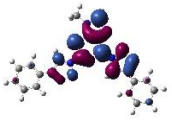	5.35	0.213
HOMO-3 (Purine acceptor) → LUMO (Purine acceptor) (LE_2)			
-6.92 eV 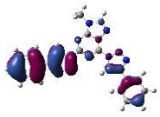	+0.14 eV 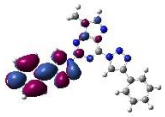	5.51	0.462
HOMO-1 ("Blue" branch donor) → LUMO+2 ("Blue" branch donor) (LE_3)			
-6.80 eV 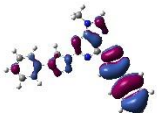	+0.28 eV 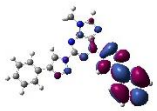	5.55	0.210
HOMO ("Red" branch donor) → LUMO+3 ("Red" branch donor) (LE_4)			

Table S4. Fundamental molecular orbitals and their energies, optical transition energies and appropriate oscillator strengths of compound **3** in optimized ground state geometry. The geometry optimization as well as optical transition properties were evaluated with DFT approximation and BMK functional at 6-31g (d,p) basis set level in vacuum.

HOMO	LUMO	Transition energy (eV)	Oscillator strength
-6.27 eV 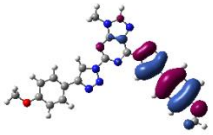	-1.44 eV 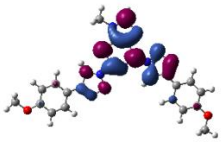	3.72	0.320
HOMO ("Red" branch donor) → LUMO (Purine acceptor) (CT_1)			
-6.40 eV 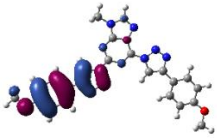	-1.44 eV 	3.97	0.270
HOMO-1 ("Blue" branch donor) → LUMO (Purine acceptor) (CT_2)			
-6.27 eV 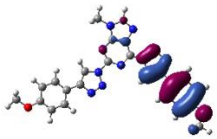	-0.617 eV 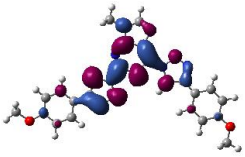	4.52	0.250
HOMO ("Red" branch donor) → LUMO+1 (Purine acceptor) (CT_3)			
-6.40 eV 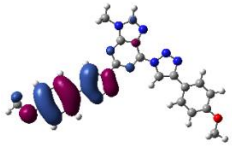	-0.617 eV 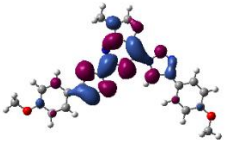	4.69	0.054
HOMO-1 ("Blue" branch donor) → LUMO+1 (Purine acceptor) (CT_4)			
-8.78 eV 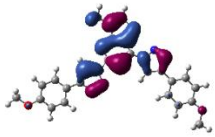	-1.44 eV 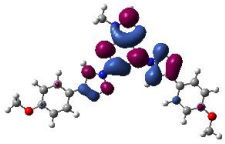	5.25	0.340
HOMO-2 (Purine acceptor) → LUMO (Purine acceptor) (LE_1)			
-6.40 eV 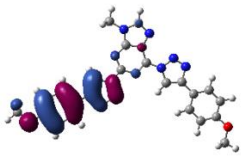	+0.42 eV 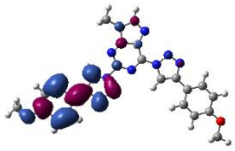	5.30	0.694
HOMO-1 ("Blue" branch donor) → LUMO+2 ("Blue" branch donor) (LE_2)			
-6.27 eV 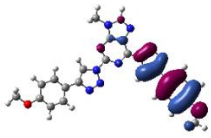	+0.56 eV 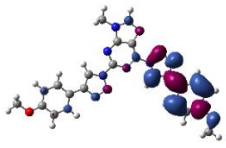	5.33	0.124
HOMO ("Red" branch donor) → LUMO+3 ("Red" branch donor) (LE_3)			

Table S5. Fundamental molecular orbitals and their energies, optical transition energies and appropriate oscillator strengths of compound **4** in optimized ground state geometry. The geometry optimization as well as optical transition properties were evaluated with DFT approximation and BMK functional at 6-31g (d,p) basis set level in vacuum.

HOMO	LUMO	Transition energy (eV)	Oscillator strength
-5.55 eV 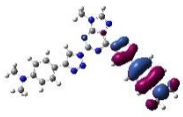	-1.26 eV 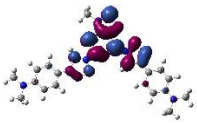	3.32	0.301
HOMO (“Red” branch donor) → LUMO (Purine acceptor) (CT_1)			
-5.67 eV 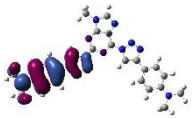	-1.26 eV 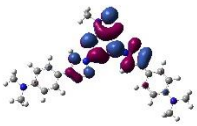	3.56	0.232
HOMO-1 (“Blue” branch donor) → LUMO (Purine acceptor) (CT_2)			
-5.55 eV 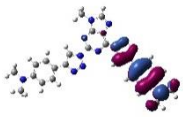	-0.40 eV 	4.19	0.238
HOMO (“Red” branch donor) → LUMO+1 (Purine acceptor) (CT_3)			
-5.67 eV 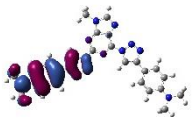	-0.40 eV 	4.28	0.074
HOMO-1 (“Blue” branch donor) → LUMO+1 (Purine acceptor) (CT_4)			
-5.67 eV 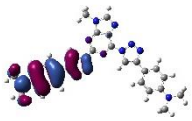	+0.68 eV 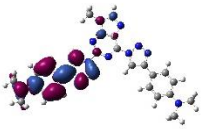	4.89	1.000
HOMO-1 (“Blue” branch donor) → LUMO+2 (“Blue” branch donor) (LE_1)			
-5.55 eV 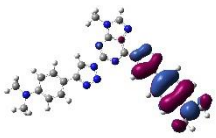	+0.82 eV 	4.96	0.283
HOMO (“Red” branch donor) → LUMO+3 (“Red” branch donor) (LE_2)			
-8.55 eV 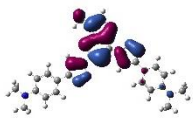	-1.26 eV 	5.70	0.263
HOMO-2 (Purine acceptor) → LUMO (Purine acceptor) (LE_3)			

Table S6. HOMO, HOMO-1, LUMO and LUMO+1 energies in an optimized ground state geometry, obtained with BMK functional at a 6-31g (d,p) basis set level in vacuum.

Compound	HOMO energy, eV		LUMO energy, eV	
1	0	-7.990	0	-1.960
	-1	-8.526	+1	-1.106
2	0	-6.795	0	-1.540
	-1	-6.924	+1	-0.725
3	0	-6.268	0	-1.439
	-1	-6.400	+1	-0.617
4	0	-5.547	0	-1.258
	-1	-5.672	+1	-0.399

5. NMR titration experiments

5.1 Titration of compound 3 with $Ca(ClO_4)_2 \bullet 4H_2O$

A reference ^1H NMR spectrum of 0.01 M solution of compound **3** (6.66 mg, 10 µmol) in CD_3CN (0.5 mL) containing benzene as internal standard was registered at 50 °C.[4]

Then $Ca(ClO_4)_2 \bullet 4H_2O$ solution containing benzene as internal standard was prepared: $Ca(ClO_4)_2 \bullet 4H_2O$ (20.0 mg, 64 µmol) and C_6H_6 (1 µL) were solubilized in CD_3CN (0.840 g, 1.00 mL, ρ = 0.84 g/mL) to obtain a solution with $[Ca^{2+}]$ 64 µmol/mL

The samples containing various ratios of compound **3** and $Ca(ClO_4)_2 \bullet 4H_2O$ were prepared as follows: compound **3** (6.82 mg, 10.2 µmol) was dissolved in CD_3CN (0.1 mL) and mixed with calculated amount of $Ca(ClO_4)_2 \bullet 4H_2O$/ C_6H_6 solution in CD_3CN ($[Ca^{2+}]$ 64 µmol/mL; step 0.025 equiv. = 0.255 µmol = 4 µL of solution). The resulting mixture was diluted with CD_3CN to the final volume 0.5 mL.

The resulting final limpid mixture was shaken, let to complex and analyzed by NMR at 50 °C (Figures S20, S21).

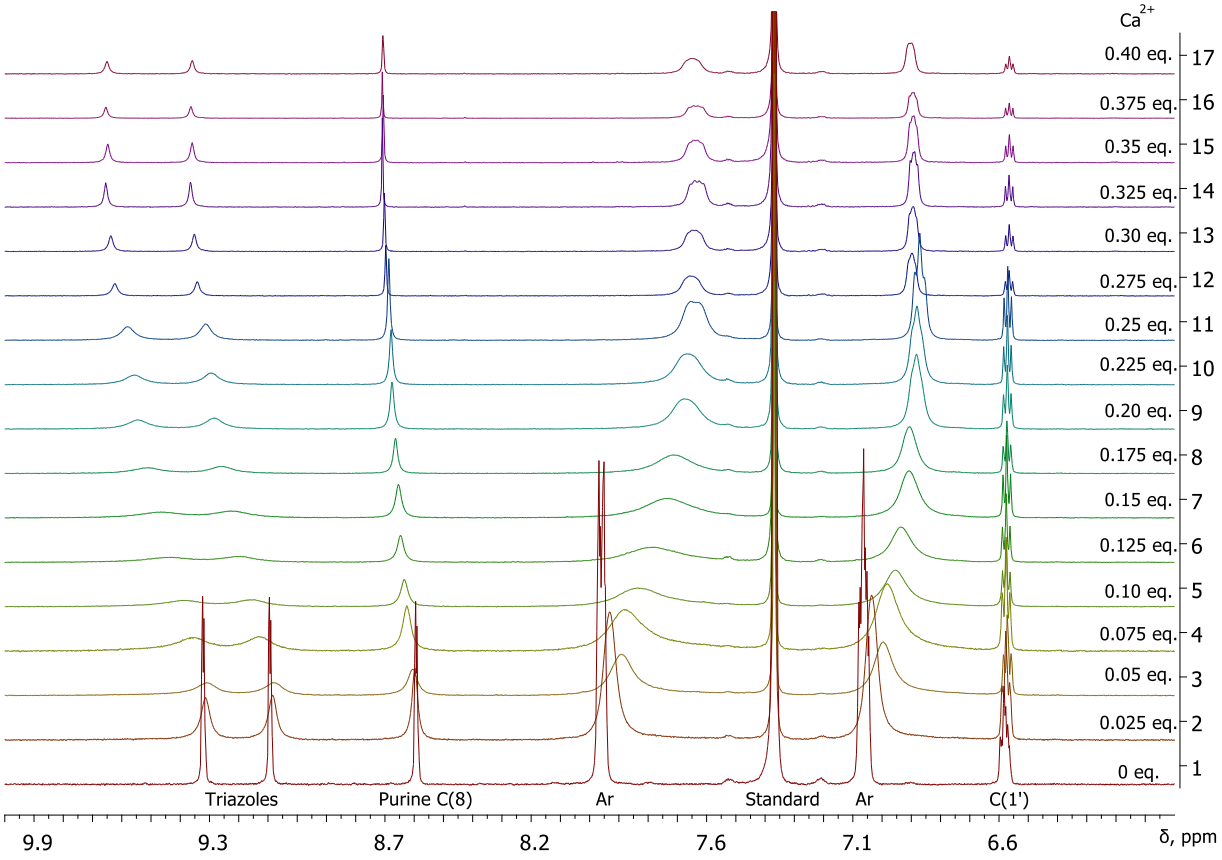

Figure S22. ^1H-NMR (500 MHz, CD_3CN with benzene as standard, 50°C) titration of compound **3** with $Ca(ClO_4)_2 \cdot 4H_2O$.

[4] Preliminary experiments at various temperatures (-20, -10, 0, 10, 20, 30, 40, 50 °C) revealed, that the complexation equilibria existing in the solution lead to intermediate exchange or even vanishing of ^1H signals at temperatures < 50 °C. Coalescence temperature was determined to be ~40 °C.

The obtained ^{1}H NMR spectra were calibrated on benzene as internal standard. For each signal its chemical shift change (Δδ, ppm) arising from the added salt was calculated. A titration curve as dependence of chemical shift change (Δδ, ppm) from the added amount of salt (molar equivalents against purine derivative **3**) was constructed (Figure S21).

Saturation of titration curves was observed at molar ratio compound **3** : $Ca(ClO_4)_2 \bullet 4H_2O$ = 3: 1

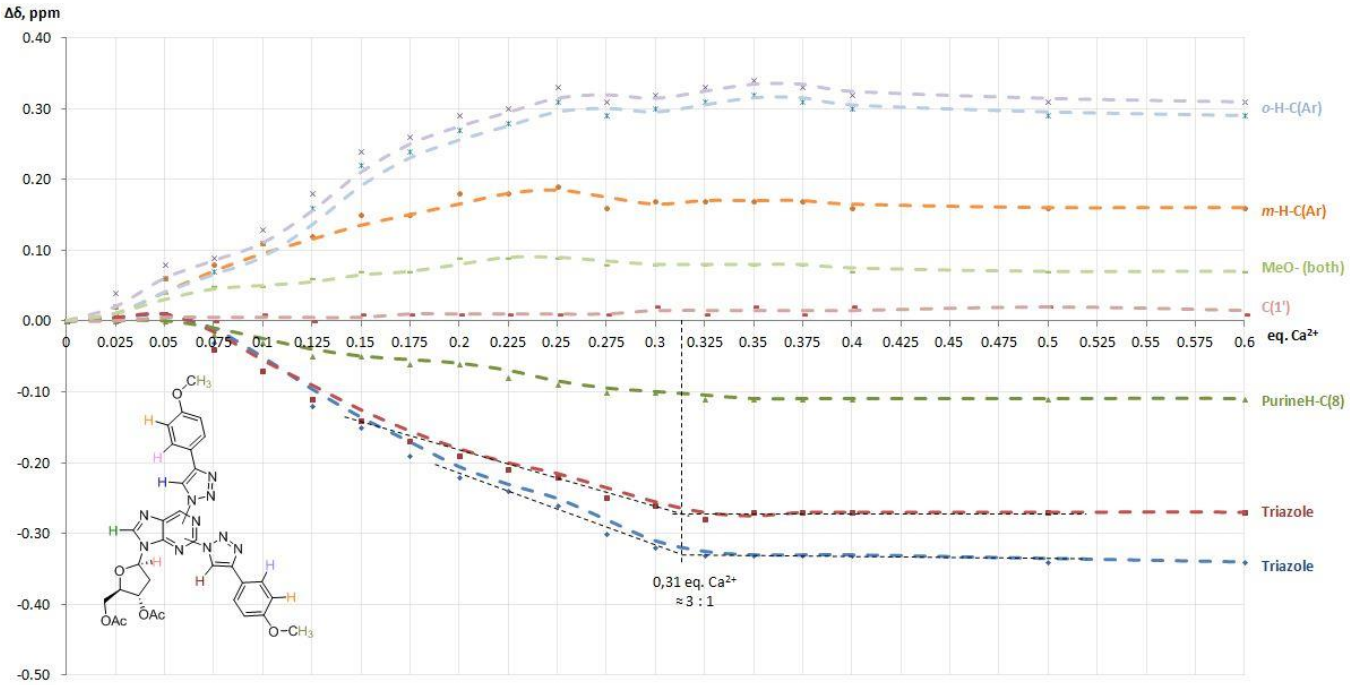

Figure S23. Chemical shift change (Δδ, ppm) as a function from added amount of $Ca(ClO_4)_2 \bullet 4H_2O$. Only the signals with significant chemical shift changes are provided.

5.2 Titration of compound 3 with $Zn(ClO_4)_2 \bullet 6H_2O$

A reference ^1H NMR spectrum of 0.01 M solution of compound **3** (6.66 mg, 10 µmol) in CD_3CN (0.5 mL) containing benzene as internal standard was registered at 50 °C.[5]

Then $Zn(ClO_4)_2 \bullet 6H_2O$ solution containing benzene as internal standard was prepared: $Zn(ClO_4)_2 \bullet 6H_2O$ (23.5 mg, 63 µmol) and C_6H_6 (1 µL) were solubilized in CD_3CN (0.840 g, 1.00 mL, ρ = 0.84 g/mL) to obtain a solution with $[Zn^{2+}]$ 63 µmol/mL

The samples containing various ratios of compound **3** and $Zn(ClO_4)_2 \bullet 6H_2O$ were prepared as follows: compound **3** (6.73 mg, 10.1 µmol) was dissolved in CD_3CN (0.1 mL) and mixed with calculated amount of $Zn(ClO_4)_2 \bullet 6H_2O$/ C_6H_6 solution in CD_3CN ($[Zn^{2+}]$ 63 µmol/mL; step 0.025 equiv. = 0.253 µmol = 4 µL of solution). The resulting mixture was diluted with CD_3CN to the final volume 0.5 mL.

The resulting final limpid mixture was shaken, let to complex and analyzed by NMR at 50 °C (Figures S22, S23).

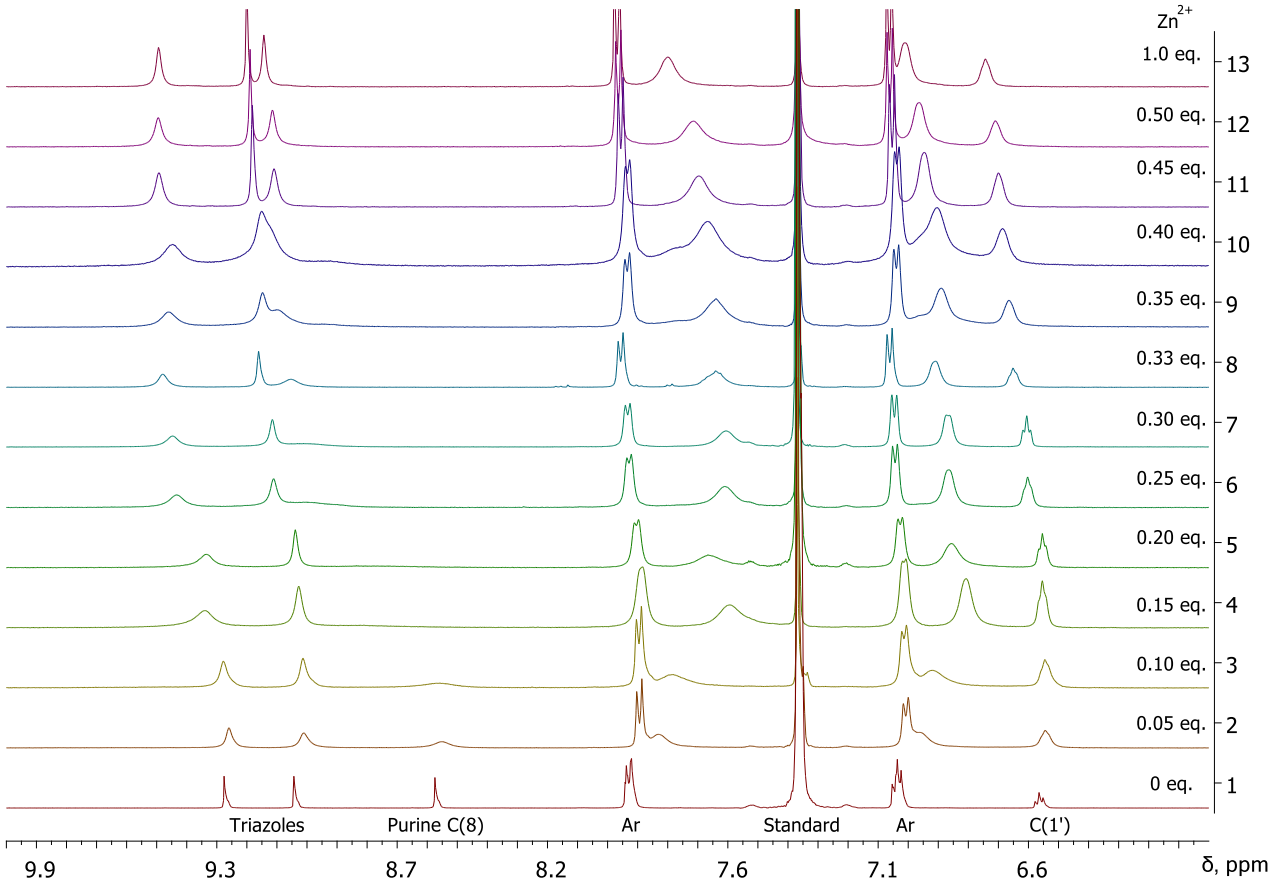

Figure S24. ^1H-NMR (500 MHz, CD_3CN with benzene as standard, 50°C) titration of compound **3** with $Zn(ClO_4)_2 \cdot 6H_2O$.

[5] Preliminary experiments at various temperatures (-20, -10, 0, 10, 20, 30, 40, 50 °C) revealed, that the complexation equilibria existing in the solution lead to intermediate exchange or even vanishing of ^1H signals at temperatures < 50 °C. Coalescence temperature was determined to be ~40 °C.

The obtained ^{1}H NMR spectra were calibrated on benzene as internal standard. For each signal its chemical shift change (Δδ, ppm) arising from the added salt was calculated. A titration curve as dependence of chemical shift change (Δδ, ppm) from the added amount of salt (molar equivalents against purine derivative **3**) was constructed (Figure S21).

Saturation of titration curves was observed at molar ratio compound **3** : $Zn(ClO_4)_2 \bullet 6H_2O$ = 3: 1

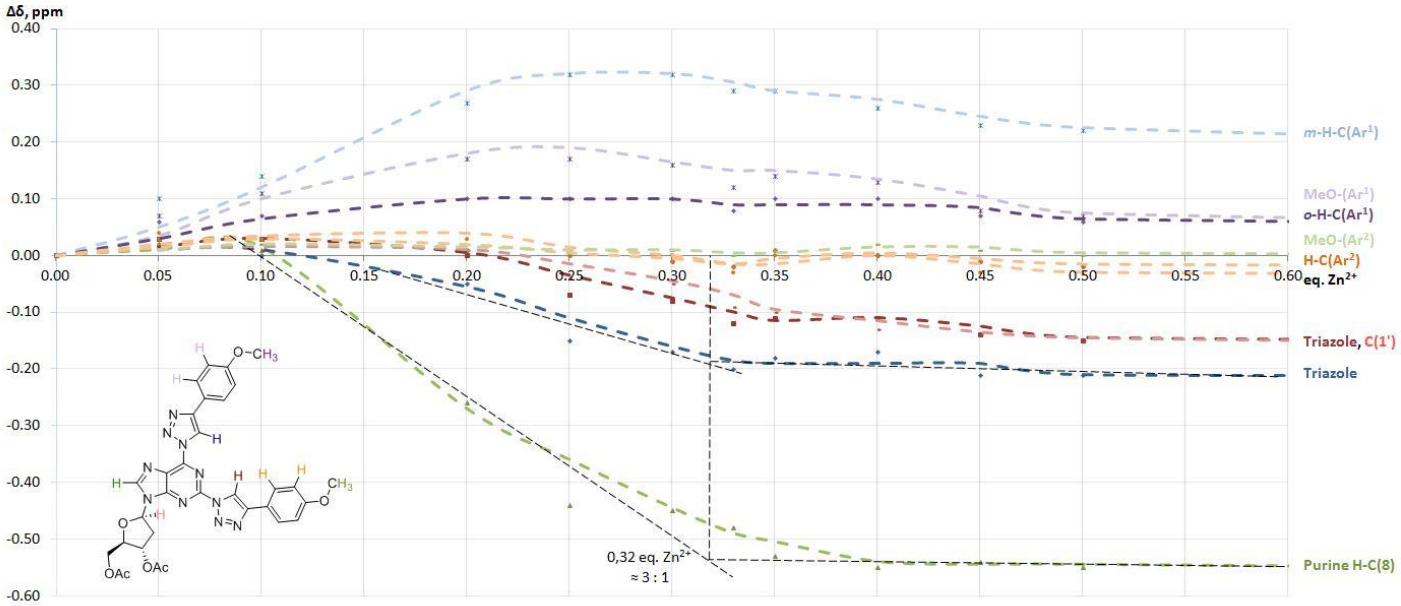

Figure S25. Chemical shift change (Δδ, ppm) as a function from added amount of $Zn(ClO_4)_2 \bullet 6H_2O$. Only the signals with significant chemical shift changes are provided.

5.3 Titration of compound 6 with $Zn(ClO_4)_2 \bullet 6H_2O$

The NMR titration experiments of 9-heptyl-6-[4-(4-methoxyphenyl)-1*H*-1,2,3-triazol-1-yl]-9*H*-purine **6** with Zn^{2+} ions were carried out. The switch to heptyl group at purine N9 position was implemented due to the solubility and stability issues. The samples were prepared according to general procedure, as previously mentioned for compound **3** (Sections 5.1 and 5.2). In this case coalescence is achieved at 25 °C.

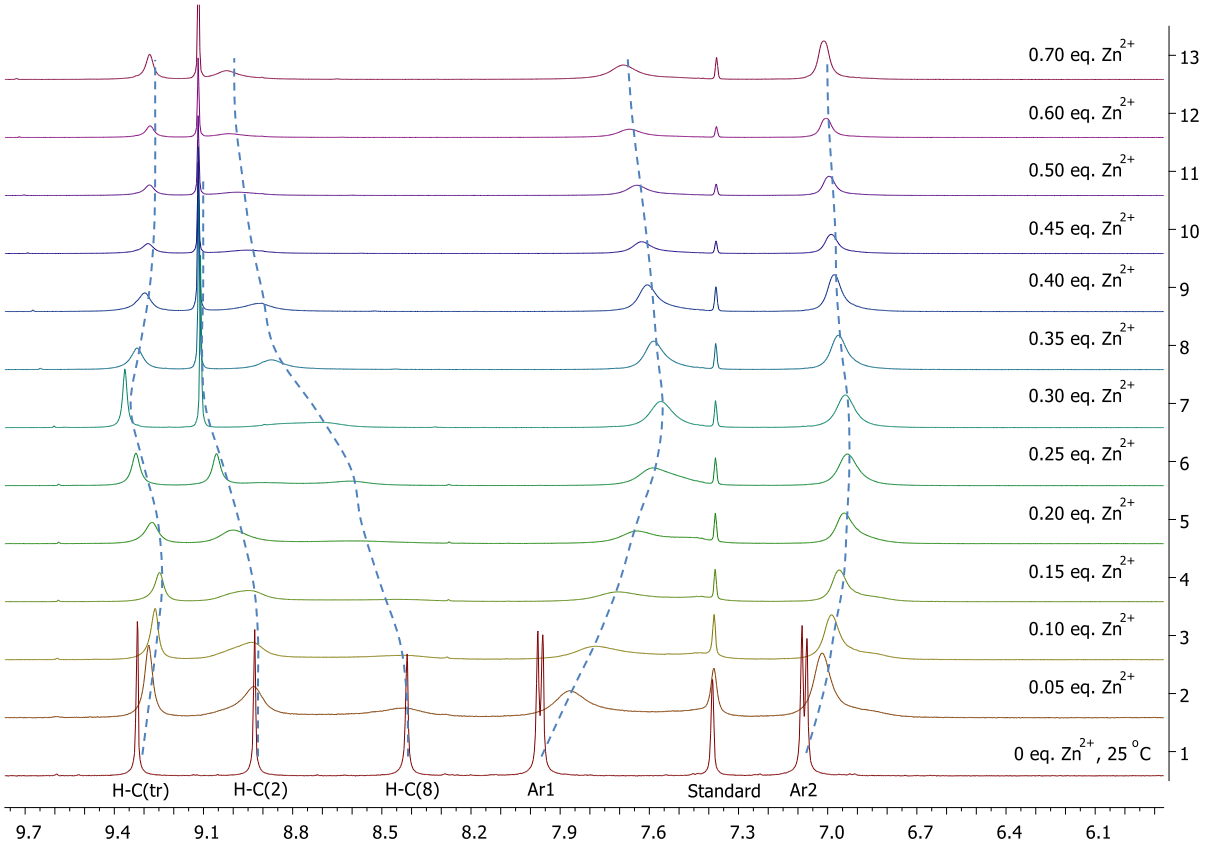

Figure S26. ^{1}H-NMR (500 MHz, CD_3CN with benzene as standard, 25°C) titration of compound **6** with $Zn(ClO_4)_2 \cdot 6H_2O$.

The considerably bigger shift change of H-C(8) and *o*-H-C(Ar) signals (0.6 and 0.4 ppm, respectively), compared to H-C(2) (0.2 ppm), leads to the same complexation pattern as previously mentioned. Compounds **3** and **6** exhibit similar complexation-induced NMR chemical shift change in the presence of Zn^{2+} ions.

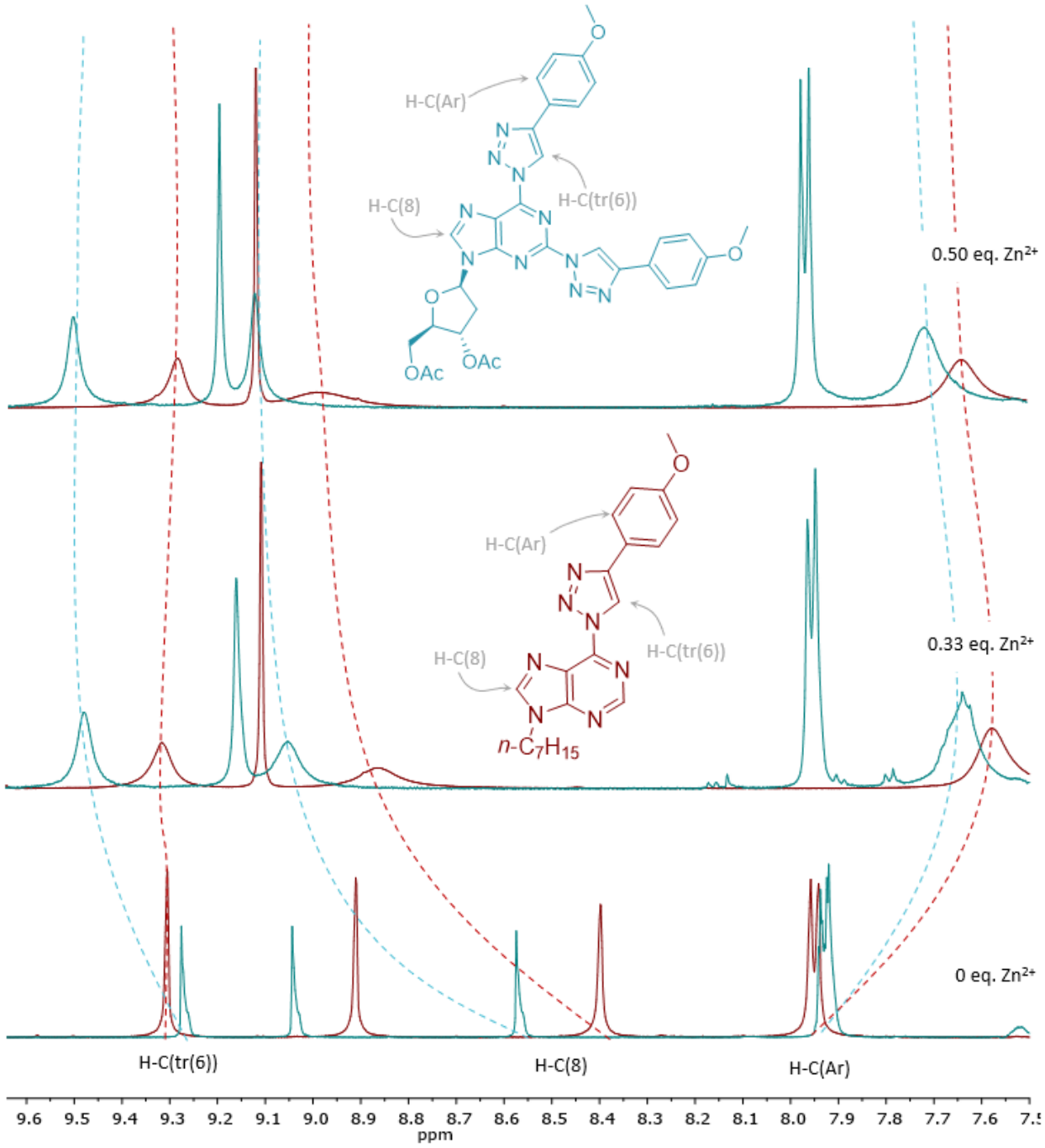

Figure S27. Comparison of NMR shifts of compounds **3** (blue) and **6** (red) during titration with $Zn(ClO_4)_2 \cdot 6H_2O$

5.4 Titration of compounds 2 and 4 with $Zn(ClO_4)_2 \bullet 6H_2O$ and $Ca(ClO_4)_2 \bullet 4H_2O$

Although metal complexes of compounds **2** and **4** showed lower emission quantum yields, the pattern of NMR signal shifts in the presence of Zn^{2+} and Ca^{2+} remains the same, as previously mentioned for compound **3** (Figures S22-S25). The samples are prepared according to general procedure (Sections 5.1 and 5.2).

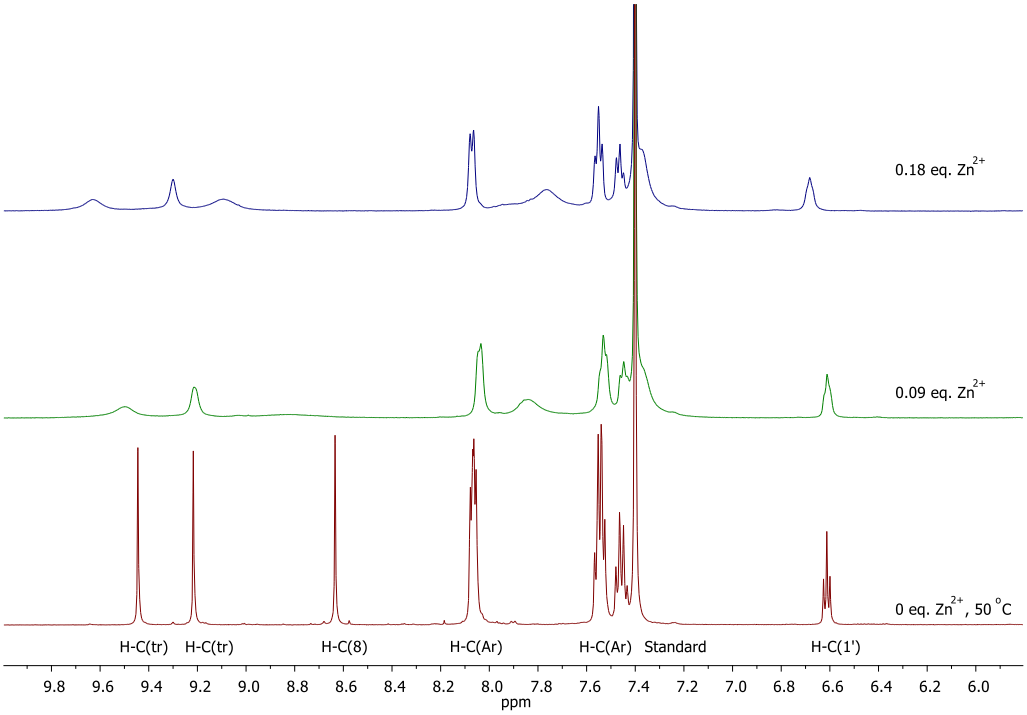

Figure S28. ^{1}H-NMR (500 MHz, CD_3CN with benzene as standard, 50°C) titration of compound **2** with $Zn(ClO_4)_2 \cdot 6H_2O$.

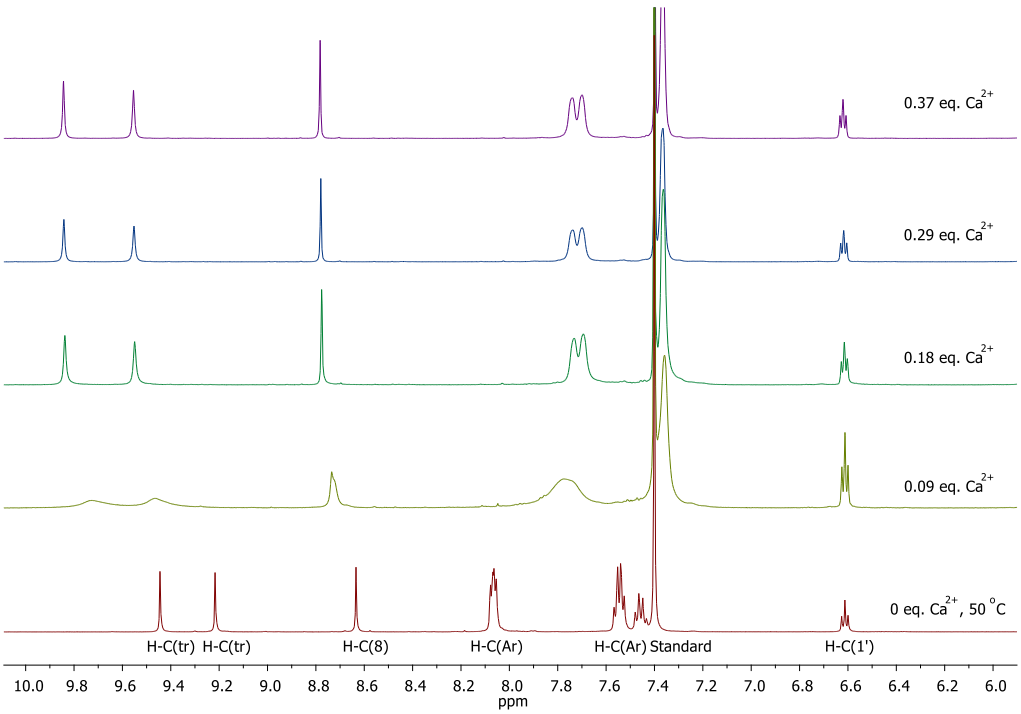

Figure S29. ^{1}H-NMR (500 MHz, CD_3CN with benzene as standard, 50°C) titration of compound **2** with $Ca(ClO_4)_2 \cdot 4H_2O$.

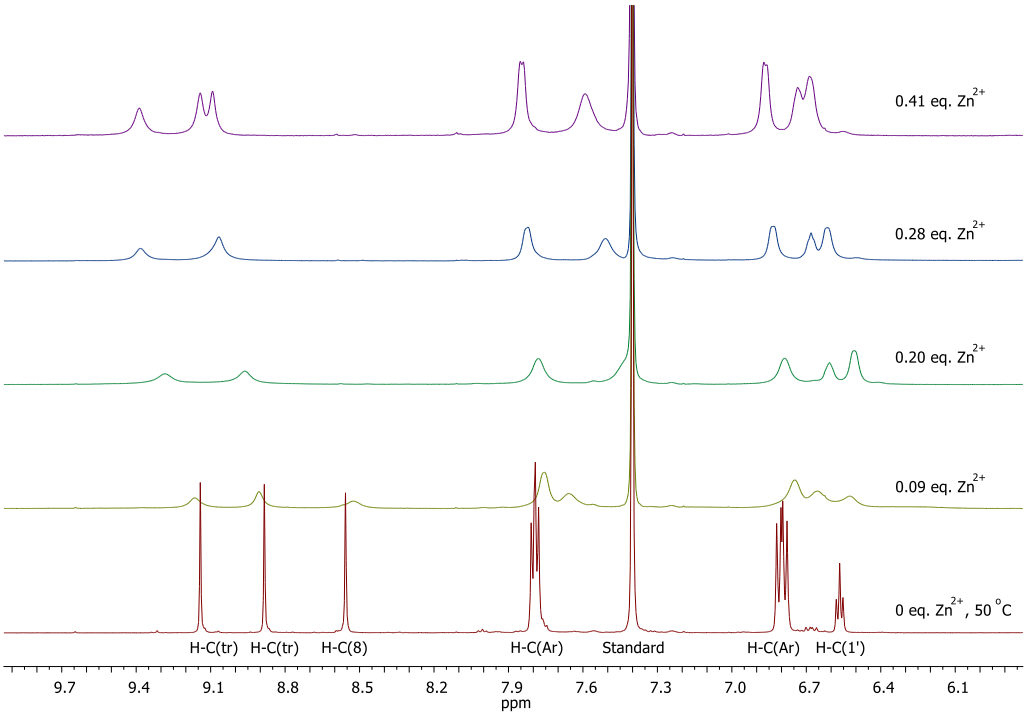

Figure S30. ^{1}H-NMR (500 MHz, CD_3CN with benzene as standard, 50°C) titration of compound **4** with $Zn(ClO_4)_2 \cdot 6H_2O$.

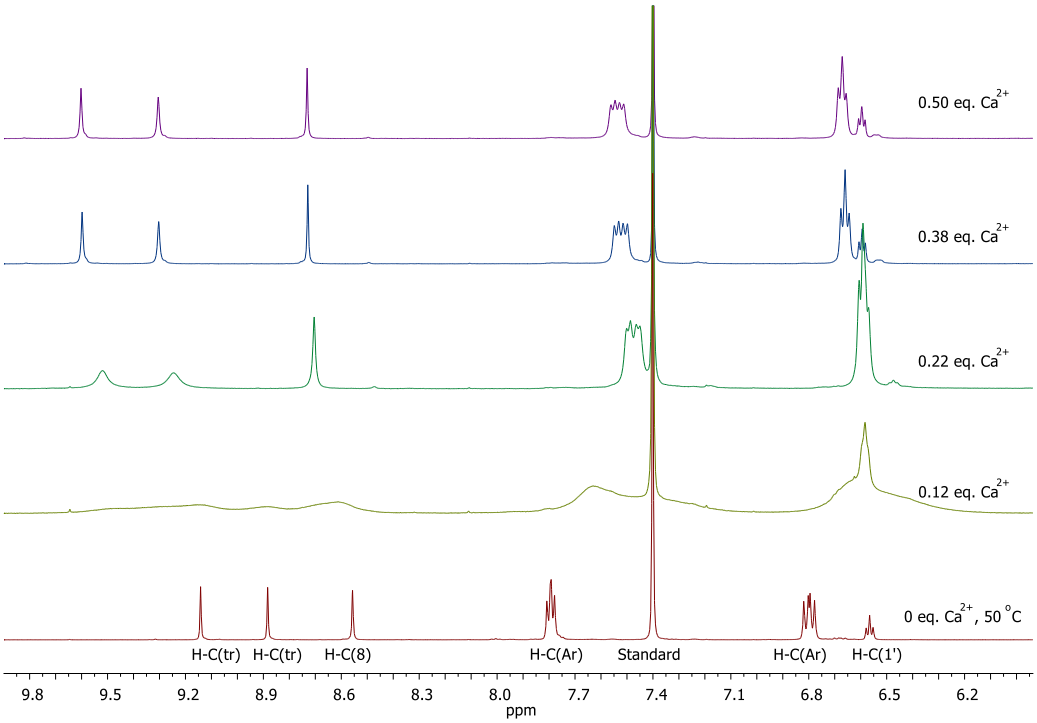

Figure S31. ^{1}H-NMR (500 MHz, CD_3CN with benzene as standard, 50°C) titration of compound **4** with $Ca(ClO_4)_2 \cdot 4H_2O$.

References

1 K. Suzuki, A. Kobayashi, S. Kaneko, K. Takehira, T. Yoshihara, H. Ishida, Y. Shiina, S. Oishi and S. Tobita, *Phys. Chem. Chem. Phys.*, 2009, **11**, 9850.

2 M. La Rosa, S. A. Denisov, G. Jonusauskas, N. D. McClenaghan and A. Credi, *Angew. Chemie*, 2018, **130**, 3158–3161.

3 K. Ozols, D. Cīrule, I. Novosjolova, D. Stepanovs, E. Liepinsh, Ē. Bizdēna and M. Turks, *Tetrahedron Lett.*, 2016, **57**, 1174-1178..

4 Z. Janeba, P. Francom and M. J. Robins, *J. Org. Chem.*, 2003, **68**, 989–992.

5 S. Ben Wang, X. Q. Deng, D. C. Liu, H. J. Zhang and Z. S. Quan, *Med. Chem. Res.*, 2014, **23**, 4619–4626.